Laboratory of Nuclear Studies, Cornell University

October 3, 2000 CBN 00-10

THE MICROWAVE UNDULATOR

Richard Talman

Laboratory of Nuclear Studies
Cornell University
Ithaca NY 14853

ABSTRACT

High order diffraction maxima from a magnetic undulator can extend the spectrum produced in a synchrotron X-ray source to high energy, but the resulting beam has (undesirably) high power relative to the flux of useful X-rays. Making the undulator period short can concentrate the beam power in the useful spectral range, but a magnetic undulator with ideal radiation properties usually has a gap height too small for satisfactory operation at existing storage rings. To overcome these limitations it is here proposed to replace the magnetic undulator field by an electromagnetic wave, propagating in a waveguide that serves also as the accelerator vacuum pipe. Because the "undulator" can pass through lattice focusing elements, it can be long yet inexpensive. For achievable microwave power, flux and brilliance can be achieved up to (almost) the limit that defines ideal undulator operation. By controlling microwave properties, the energy, flux, and state of polarization of the X-ray beam can be tuned (within microseconds) independent of storage ring parameters, and without disrupting the circulating beam. The controls for these parameters can therefore be put in the hands of the separate experimenters in separate beam lines. A possible design is given for an X-ray source centered on 12.4 keV X-ray energy, along with numerical estimates of its expected performance at the Cornell Electron Storage Ring (CESR), modified to maximize brilliance, and running at 5.1 GeV. The radiation from this system is analysed both classically, as undulator radiation, and quantum mechanically, as Compton scattering.

1. Introduction

The narrow band of energies, mentioned in the abstract as being ideal for X-ray diffraction, is limited on the high energy side by difficulty in making optical elements in that range, by excessive heating, by longterm damage, and by unwelcome backgrounds. The low energy limit is due to excessive attenuation in vacuum windows, protective covers and thick samples. The attenuation length of few keV photons is so short as to cause unacceptable attenuation but, because of the extremely rapid energy dependence of attenuation length, a factor of ten increase in energy largely overcomes this problem. One therefore seeks a photon beam centered on, say, $E_\gamma = 12.4\,\mathrm{keV}$,[†] as brilliant as possible, consistent with being as monochromatic as possible. The use of undulators to produce beams of this sort at electron storage rings is by now well understood, but the undulator period is too short to be practical for most storage rings. The apparatus proposed in this paper is intended to supercede such an undulator in order to produce a beam that has brilliance, large both on an absolute basis and relative to total beam power, and is non-intrusive on the circulating beam.

The qualitative idea behind undulator radiation is familiar from the pattern produced by an optical diffraction grating, having multiple slits. Individual slits that are extremely thin and closely spaced produce single slit diffraction patterns that are very broad in angle and very nearly superimposed. As a result there is interference, which causes angular maxima and minima. The angular widths of the maxima are inversely proportional to the number of slits and, instead of being spread more or less uniformly in angle, the energy getting through the slits is concentrated in these maxima.

The primary element of a conventional undulator is a magnet having many, say, $2N_w$ magnetic poles, alternately north and south, with period λ_w. The trajectory of an electron through this magnet oscillates transversely about a straight central line, and this transverse acceleration of the electron results in synchrotron radiation. Though the radiation from different electrons is incoherent, the waves emitted from the same electron in different deflections interfere coherently. The fundamental interference maximum occurs when (because of the electrons speed deficit relative to c) the electron lags the radiated field

[†] The choice of $E_\gamma = 12.4\,\mathrm{keV}$ as nominal energy corresponds to a wavelength $\lambda_\gamma = 1\mathring{A}$ and to the (mnemonic) approximation $1\mathring{A} \to 12345\,\mathrm{eV}$.

by exactly one wavelength in passing through one period of the undulator. (Neglecting angular dependence and path length excess) this yields a condition

$$\lambda_\gamma = \frac{\lambda_w}{2\gamma^2} \ , \tag{1.1}$$

giving λ_γ, the short wavelength edge of the first order diffraction maximum, in the ideal limit of undulator operation. For numerical estimates in this paper the value $\gamma = 10^4$, corresponding to 5.1 GeV operation, will be assumed. Then the choice $\lambda_w = 2\,\mathrm{cm}$ yields $\lambda_\gamma = 1.0\,\text{Å}$, or about 12.4 keV.

Unfortunately it is typically impractical for λ_w to be this small because of the inevitable fringing between the poles and a correspondingly too-small gap height requirement. One can contemplate using higher order interference maxima but, since the electron's trajectory through a standard undulator is essentially sinusoidal, the higher orders are extremely weak. The apparatus proposed to overcome this limitation is shown in Fig. 1.1.

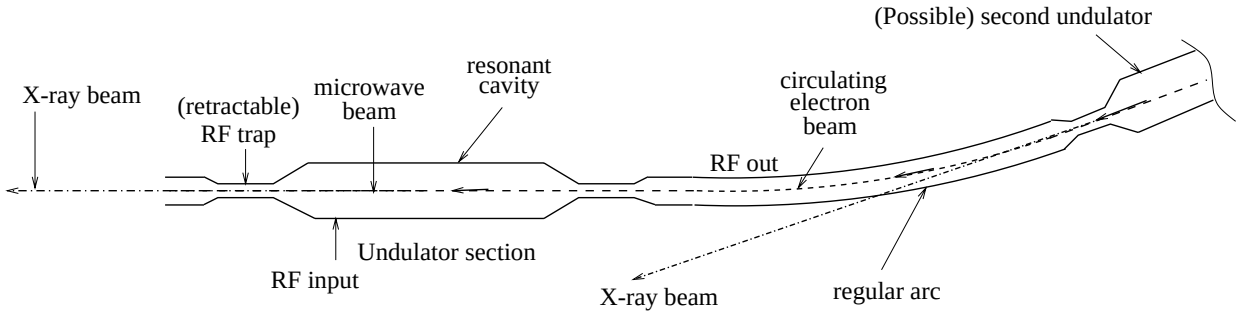

Figure 1.1: Microwaves in the "undulator" collide with circulating electrons. The useful microwaves propagate approximately anti-parallel to the electrons.

As illustrated also in Fig. 1.2 our *microwave undulator* consists of a powerful microwave beam, propagating in a rectangular waveguide, through which the bunch of electrons or positrons passes. Depending on the propagation mode in the waveguide and whether the beam is a traveling or a standing wave, the microwave beam can be idealized as a superposition of two, four, or eight monochromatic plane waves. There is a close analogy between a conventional magnetostatic undulator and a standing wave beam, since the spatial dependence of their deflecting fields (at fixed time) are the same. But, to the extent the electron and microwave beams are parallel, the transverse force due to the parallel-traveling beams are negligible (because electric and magnetic forces cancel) and, to

calculate the X-ray production, it is only necessary to consider the anti-parallel microwave beam. Any one of these anti-parallel fields is characterized by "guide wavelength" λ_g, and its fields depend on position and time as $\cos(2\pi z/\lambda_g - \omega_{\rm rf} t)$. For an electron whose position is given by $z = -vt$ (where $v \approx c$) the field dependence is $\cos((2\pi/\lambda_g + \omega_{\rm rf}/v)z)$, which implies

$$\frac{1}{\lambda_w} = \frac{1}{\lambda_g} + \frac{\omega_{\rm rf}/\left(2\pi\right)}{v} \approx \frac{1}{\lambda_g} + \frac{1}{\lambda_{\rm rf}} \ , \tag{1.2}$$

yielding "effective wiggler wavelength" λ_w in terms of λ_g and "free space wavelength" $\lambda_{\rm rf}$. For waves traveling approximately parallel to the guide axis, this yields $\lambda_w \approx \lambda_{\rm rf}/2$. So our nominal 12.4 keV energy, requires an RF generator yielding free space wavelength $\lambda_{\rm rf} \approx 2\lambda_w = 4\,{\rm cm}$, i.e. $7.5\,{\rm GHz}$.

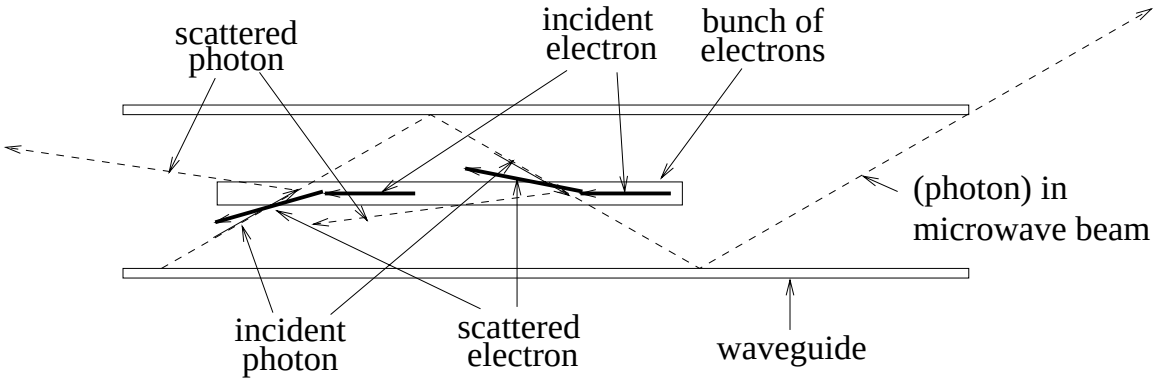

Figure 1.2: Microwave undulator configuration. An electron beam collides with a traveling (or standing) microwave beam. The microwave beam can be thought of as a superposition of plane waves that reflect repeatedly off the conducting walls of the waveguide.

For purposes of estimating X-ray beam fluxes using traveling waves, we can use traditional undulator formulas with undulator period given by Eq. (1.2). In this picture the microwave beam is treated (classically) as an external force field that causes electrons to oscillate transversely. The analysis of the next few sections will therefore apply equally to conventional undulators and wigglers, and language from the latter field will be employed.† Later, when the radiation is calculated quantum mechanically, the microwave beam will have to be treated as the appropriate superposition of plane waves.

† In fact, the next few sections amount to being a tutorial on convevtional undulators.

2. Synchrotron Radiation From a "Short" Deflector

The following treatment of undulators is intended to complement the treatment in Jackson. Working in the rest frame of the electron, Jackson evaluates the radiation from a transversely oscillating dipole, and from that the angular distribution of (monochromatic) photons in that frame. To find the laboratory distribution (no longer monochromatic, but with wavelength dependent on angle) he Lorentz transforms individual photons into the laboratory frame. (I think this analysis may be due to Hoffmann originally.) The present treatment, Maxwellian, and without making explicitly relativistic arguments, will proceed entirely in the laboratory frame. My motivation is two-fold. One is to develop and exploit the analogy between undulators and diffraction gratings; for this it is necessary to represent the undulator as a sequence of $2N_w$ short, alternating-sign, deflectors, rather than as harmonic oscillation. My other motive is to investigate certain features of Jackson's treatment that appear to contradict part of the lore of the field. I refer here to the "angular narrowing" of the forward peak, making its angular width proportional to $1/\sqrt{N_w}$, as described initially by Attwood, Halbach, and Kim.[1] This feature is (superficially) absent from Jackson's result. Since I will be satisfied with semi-quantitative features, I will not hesitate to make fairly crude approximations.

The fundamental relationship governing synchrotron radiation is between observation time t and "retarded time" t_r:

$$t = t_r + \frac{\varsigma}{c} \ , \tag{2.1}$$

where ς is the distance from source point to observation point P. Approximating formulas from Jackson[2] fairly radically, the electric field at P, due to an electron traveling in a circle of radius R is

$$E_x\left(\mathbf{r},t\right) \approx \frac{q}{4\pi\epsilon_0}\,\frac{4\gamma^4}{\varsigma R}\left(1+\gamma^2\,\psi^2+\left(\frac{2c\,\gamma^3/R}{1+\gamma^2\,\psi^2}\right)^2\,t^2\right)^{-2}\left(U\left(t-t_{\rm in}\right)-U\left(t-t_{\rm out}\right)\right) \ . \tag{2.2}$$

This field is appreciable only for emission directions within a range of vertical angles $|\psi|\tilde{<}1/\gamma$ about a central peak and for a correspondingly short time interval, centered on the time $t = 0$ when the electron's velocity vector points toward P. The final factor $U(t - t_{\rm in}) - U(t - t_{\rm out})$ is a "window function", equal to 1 when the electron is being deflected and zero otherwise. This factor is needed if the deflection interval is "short",

$L < 2R/\gamma$, which will be the case in this paper; even though the true longitudinal field dependence is sinusoidal, deflection from each half period will be treated as a short impulse.

Three important approximations have been made in obtaining Eq. (2.2). Fortunately, the least-controlled of these approximations, namely dropping a term proportional to t_r^3 in the relation between retarded time t_r and observation time t, is valid for short magnets. This is because, being cubic, the excess length of a curved path in a short magnet is even less important than in a long magnet, relative to the effects of vertical angle and electron speed deficit. Another approximation in Eq. (2.2) amounts to having neglected vertically polarized radiation altogether. For "in-plane" radiation this is an excellent approximation, but as much as 20% of "out-of-plane" radiated intensity can be vertically polarized. The same approximation causes Eq. (2.2) to over-estimate the horizontally polarized intensity by a similar amount.

We will be prepared to make an even more extreme approximation, that will be valid in the pure undulator regime. Suppose the "window function" is non-vanishing for a time so short that the angle subtended by the electron's velocity vector is small compared to ψ. Then, in Eq. (2.2), we can make the replacement

$$\gamma^2\,\psi^2 + \left(\frac{2c\,\gamma^3/R}{1+\gamma^2\,\psi^2}\right)^2\,t^2 \to \gamma^2\,\vartheta^2 \tag{2.3}$$

where ϑ is the polar angle relative to the beam axis. The basis of this approximation is that, with the electron's angle being treated as constant, the t^2 term can be dropped, and the retarded time correction becomes azimuthally symmetric. Since this approximation is rather drastic, it should be applied only when strictly necessary. (It will be useful when discussing the angular width of the forward peak produced by a multiperiod undulator in the pure undulator limit.)

It will simplify the calculations greatly (especially in cases where the total undulator length is comparable with the distance to the observation point) if we can suppose that the deflecting element is "very short", in the sense just explained. In fact, as well as being short, to avoid the need for step functions, the deflecting field will be taken to have

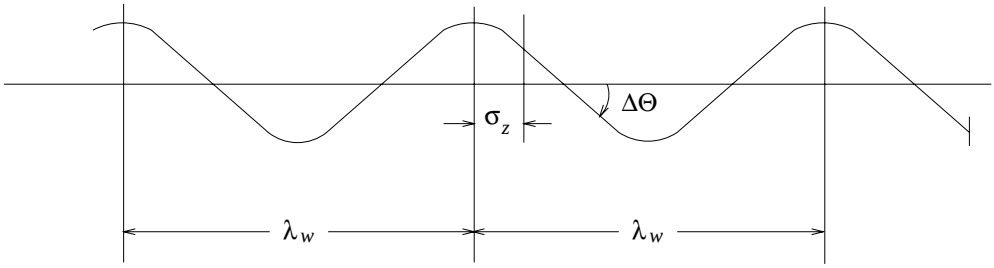

Figure 2.1: The electron orbit through the undulator is treated as a sequence of impulses, each bending through $2\Delta\Theta$, with $\Delta\Theta << 1/\gamma$, i.e. small compared to the synchrotron radiation cone angle.

Gaussian longitudinal profile such that the inverse bending radius is given by†

$$\frac{1}{R\left(z\right)} = \frac{1}{R_w}\,\exp\left(\frac{-z^2}{2\sigma_z^2}\right). \tag{2.4}$$

In passing one quarter of a wiggler period, an electron's angular deflection is

$$\Delta\Theta = \frac{1}{R_w}\int_0^\infty \exp\left(\frac{-z^2}{2\sigma_z^2}\right) dz = \sqrt{\frac{\pi}{2}}\,\frac{\sigma_z}{R_w} \equiv \frac{K_{\rm eff}}{\gamma}\ , \tag{2.5}$$

where the "effective wiggler strength parameter" $K_{\rm eff}$ has been introduced to facilitate comparison with magnetic undulators for which the maximum orbit angle relative to the undulator center line is traditionally defined as K/γ. The actual, sinusoidal, orbit, having maximum slope K/γ, is given by

$$x = \frac{\lambda_w}{2\pi}\,\frac{K}{\gamma}\,\cos\frac{2\pi\,z}{\lambda_w}\ , \quad \text{or} \quad \frac{1}{R\left(z\right)} = \frac{2\pi}{\lambda_w}\,\frac{K}{\gamma}\,\frac{\cos\left(2\pi z/\lambda_w\right)}{\left(1+K^2\sin^2\left(2\pi z/\lambda_w\right)\right)^{3/2}}\ , \tag{2.6}$$

where the latter relation is obtained from a standard formula for curvature. This curve will be matched approximately by choosing R_w and σ_z appropriately, using the approximation

$$\sin x \approx -\sum_{i=-\infty}^{\infty}\left(-1\right)^i \exp\left(-\frac{\left(x+\left(2i+1\right)\pi/2\right)^2}{2}\right)\ . \tag{2.7}$$

This is illustrated in Fig. 2.2, and the parameters are related by

$$\sigma_z = \frac{\lambda_w}{2\pi} = \frac{1}{2\pi}\,\frac{\lambda_g\lambda_{\rm rf}}{\lambda_g+\lambda_{\rm rf}}\ . \tag{2.8}$$

For our nominal 12.4 keV energy, $\sigma_z = 1/\pi$ cm. In practice, we anticipate $\lambda_g \approx \lambda_{\rm rf}$ and therefore $\sigma_z \approx \lambda_{\rm rf}/(4\pi)$.

† What with fringe fields being inevitable, treating the field shape of a short magnet as Gaussian could provide an accurate approximation, but we are intending to apply these formulas to a sinusoidal deflection field.

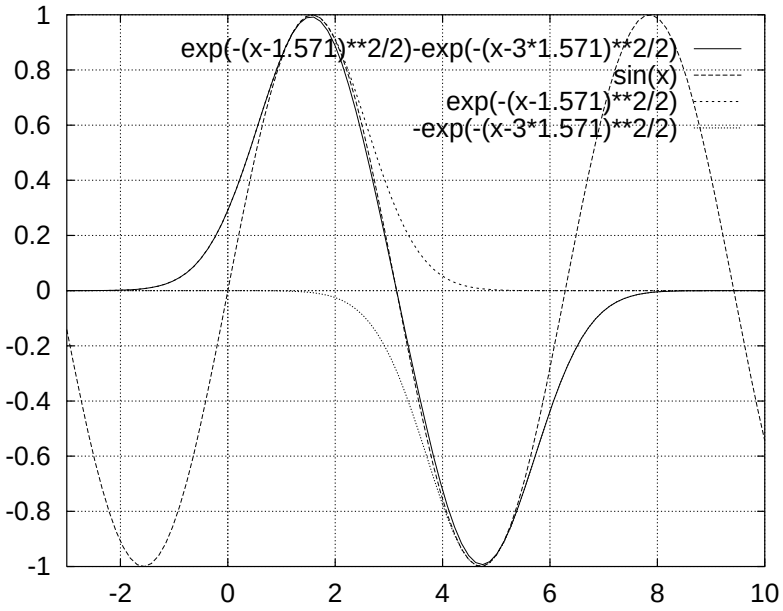

Figure 2.2: Plot illustrating a sinusoid matched by a series of alternate sign Gaussians, of which only two are shown. See key in upper right for analytic forms. The standard deviations are related to undulator wavelength by $2\pi\sigma_z = \lambda_w$ in order to match curvatures at the peaks. Though the true trajectory is sinusoidal, radiation integrals will be based on the Gaussian pulses, so radiation deficiency or excess from the tail regions will require (modest) correction.

With this (somewhat unconventional) approximation, the ends of the undulator can be represented by simply truncating the sum in Eq. (2.7). Also, after having sliced the undulator longitudinally, coherent superposition can be handled by the vector addition of phasors, one per deflection arc, or $2N_w$ in all. By using a Gaussian shape, the artificial high frequency components that would accompany using truncated half-sinusoids are largely suppressed. For long undulators it may be necessary to incorporate longitudinal dependency by making the phasor magnitude depend on longitudinal position. The electron orbit will otherwise be treated as a straight line, with longitudinal velocity altered to account for the increased arc length of the actual (sinusoidal) orbit;

$$\frac{\overline{v}}{c} \approx \sqrt{\frac{v^2}{c^2} - \overline{(\Delta\Theta \cos k_w z)^2}} \approx 1 - \frac{1}{2\gamma^2} - \frac{\Delta\Theta^2}{4}. \tag{2.9}$$

According to Sands[3] the energy dissipated per unit length in a region with bending radius R_0 is given by†

$$\frac{dU}{dz} = \frac{q^2\gamma^4}{6\pi\epsilon_0 R_0^2} \ . \tag{2.10}$$

This is sometimes known as "Schott's formula", though it is due to Liénard. The energy U_1 radiated by an electron in traversing the thin element is therefore given by

$$U_1 = \frac{q^2\gamma^4}{6\pi\epsilon_0 R_w^2} \int_{-\infty}^{\infty} \exp\left(\frac{-z^2}{\sigma_z^2}\right) dz = \frac{\sqrt{\pi}}{6\pi} \frac{q^2\gamma^4}{\epsilon_0} \frac{\sigma_z}{R_w^2} \ . \tag{2.11}$$

This can be compared to the more accurate result obtained using the second of Eqs. (2.6);

$$\begin{aligned} U_1' &= \frac{q^2\gamma^4}{6\pi\epsilon_0} \frac{2\pi}{\lambda_w} \frac{K^2}{\gamma^2} 2 \int_0^{\lambda_w/4} \frac{\cos^2\left(2\pi z/\lambda_w\right)}{\left(1 + K^2 \sin^2\left(2\pi z/\lambda_w\right)\right)^3} d\left(\frac{2\pi z}{\lambda}\right) \\ &= \frac{\pi^2/4}{6\pi} \frac{q^2\gamma^4}{\epsilon_0} \frac{\sigma_z}{R_w^2} + O\left(K^4\right) \ , \end{aligned} \tag{2.12}$$

where λ_w has been replaced using Eq. (2.8), K and K_{eff} have been equated, and the last of Eqs. (2.5) has been used. Since $\sqrt{\pi}/(\pi^2/4) = 0.72$ our formulas will underestimate the total energy radiated by this factor (which is comparable to the over-estimate built into Eq. (2.2).) This defect could be rectified by altering the definition of R_w or σ_z but I prefer to maintain the definitions given so far. Also, to permit working in terms of familiar quantities, U_1 will be expressed as a fraction of U_0 (the energy radiated as an electron travels in a complete circle of radius R_0)

$$\frac{U_1}{U_0} = \frac{R_0}{2\pi R_w^2} \int_{-\infty}^{\infty} \exp\left(-\frac{z^2}{\sigma_z^2}\right) dz = \frac{1}{2\sqrt{\pi}} \frac{R_0\,\sigma_z}{R_w^2} = \frac{1}{\pi^{3/2}} \frac{R_0}{\sigma_z} \Delta\Theta^2 \ . \tag{2.13}$$

The essential qualitative feature of this formula is that, with undulator period held fixed, the radiation comes in $2N_w$ pulses of energy, each with energy given by Eq. (2.13). All that remains is to determine how this energy is distributed in direction and wavelength.

Another formula from Jackson[2] gives the Fourier-transformed radiation field due to an electron in a uniform magnetic field to be

$$\frac{\widetilde{\mathbf{E}}_x\left(\omega,\psi\right)}{\frac{q}{4\pi\epsilon_0 c\varsigma}} \approx \ -\frac{c}{R} \frac{\omega}{\sqrt{2\pi}} \int_{-\infty}^{\infty} t_r\, e^{i\omega t_r\left(\frac{1}{2\gamma^2} + \frac{\psi^2}{2} + \frac{c^2 t_r^2}{6R^2}\right)} dt_r \ , \tag{2.14}$$

† Eq. (2.10) gives the energy radiated as a 5.1 Gev electron travels in a complete circle of radius $R_0 = 89\,\text{m}$, to be $U_0 = 0.67\,\text{MeV}$. Some numerical estimates in this paper will be scaled to U_0. Though this is artificial, it has mnemonic value, since it relates quantities to that feature of synchrotron radiation which imposes itself most emphatically upon the operation of storage rings—the average energy loss. For accurate calculation one should use $U_0 R_0 = C_\gamma E^4$, where $C_\gamma = 0.885 \times 10^{-4}\,\text{m/GeV}^3$.

where we have again suppressed vertical polarization.

Because this formula is valid only for long, uniform magnets, it needs to be adapted for our short deflection region. We will exploit the short magnet approximation by treating the shape of the angular radiation pattern, both horizontal and vertical, as constant over the time interval during which it is nonvanishing at observation point P. As stated previously, this amounts to dropping the term with t_r^2 in the exponent and making the replacement $\psi \to \vartheta$. After modifying Eq. (2.14) by moving the $1/R_0$ inside the integral, to account for variable radius, it becomes (temporarily introducing $\sigma_{t_r} = \sigma_z/c$)

$$\begin{aligned}
\frac{\widetilde{\mathbf{E}}_x(\omega,\vartheta)}{\frac{q}{4\pi\epsilon_0 \varsigma}} &\approx -\frac{i\omega}{R_w}\sqrt{\frac{2}{\pi}}\int_0^\infty t_r \exp\left(\frac{-t_r^2}{2\sigma_{t_r}^2}\right)\sin\left(\omega t_r\left(\frac{1}{2\gamma^2}+\frac{\vartheta^2}{2}\right)\right)dt_r \\
&= -\frac{i\omega}{R_w}\sqrt{\frac{2}{\pi}}\left(\frac{1}{2\gamma^2}+\frac{\vartheta^2}{2}\right)^{-2}\int_0^\infty t\exp\left(\frac{-t^2}{2\sigma_{t_r}^2\left(\frac{1}{2\gamma^2}+\frac{\vartheta^2}{2}\right)^2}\right)\sin\omega t\,dt\ . \\
&= -\frac{i\omega}{R_w}\sqrt{\frac{2}{\pi}}\,\sigma_{t_r}^2\omega_\vartheta^2\int_0^\infty t\,e^{\frac{-\omega_\vartheta^2 t^2}{2}}\sin\omega t\,dt \quad \text{where} \quad \omega_\vartheta = \frac{c}{\sigma_z}\left(\frac{1}{2\gamma^2}+\frac{\vartheta^2}{2}\right)^{-1} \\
&= -\frac{i}{R_w}\frac{\sigma_z^2}{c^2}\frac{\omega^2}{\omega_\vartheta}\exp\left(\frac{-\omega^2}{2\,\omega_\vartheta^2}\right)
\end{aligned} \tag{2.15}$$

The shape of this function is shown in Fig. 2.3. We can regard the $\vartheta = 0$ value of ω_ϑ,

$$\omega_0 = \frac{2\gamma^2 c}{\sigma_z} \tag{2.16}$$

as a frequency typical of the radiation. It can play a role much like $\omega_c = (3/2)c\gamma^3/R_0$, the "critical frequency" traditionally defined for synchrotron radiation from bend radius R_0.† (For magnetic wigglers there is some point to evaluating ω_c from the peak magnetic field but, for the undulator we are discussing, ω_c is unrelated to the radiation spectrum.) The maximum of the single deflector Fourier transform can be seen to be at $1.45\,\omega_0$. It will prove to be significant that the spectrum depends on ϑ only through the parameter ω_ϑ, so all angular dependence of the spectrum is entirely parameterized by the relation

$$\omega_\vartheta = \frac{\omega_0}{1+\gamma^2\vartheta^2}\ , \tag{2.17}$$

† Because of its stronger dependence on γ one might be misled into believing that ω_c corresponds to a more "Lorentz contracted" and hence shorter wavelength than λ_0, but this is wrong. In fact, the "short magnet effect" make the opposite true in a true undulator.

which gives the frequency width as a function of angle. The energy is distributed according to

$$\frac{d^2U_1}{d\omega d\Omega} = \frac{2\varsigma^2}{\mu_0 c}\,\tilde{E}_x\left(\omega\right)\tilde{E}_x\left(-\omega\right) = \frac{2\varsigma^2}{\mu_0 c}\left(\frac{q}{4\pi\epsilon_0\varsigma}\right)^2\left(\frac{\sigma_z^2}{R_w c^2}\right)^2\frac{\omega^4}{\omega_\vartheta^2}\exp\left(-\frac{\omega^2}{\omega_\vartheta^2}\right)\ . \tag{2.18}$$

where the factor 2 accounts for restriction of ω to positive values. The second moment of ϑ is given by

$$\sigma_\vartheta^2\left(\omega\right) = \frac{\int_0^\infty \vartheta^3\left(1/\gamma^2+\vartheta^2\right)\exp\left(-\frac{\omega^2\left(1/\gamma^2+\vartheta^2\right)}{\omega_0^2/\gamma^2}\right)d\vartheta}{\int_0^\infty \vartheta\left(1/\gamma^2+\vartheta^2\right)\exp\left(-\frac{\omega^2(1/\gamma^2+\vartheta^2)}{\omega_0^2/\gamma^2}\right)d\vartheta}\ . \tag{2.19}$$

As a check on the consistency of our formulas we calculate the total energy per deflection to be

$$\begin{aligned} U_1'' &= \frac{\varsigma^2}{\mu_0 c}\int d\Omega\int d\omega\,\tilde{E}_x\left(\omega\right)\tilde{E}_x\left(-\omega\right) \\ &= 2\,\frac{\varsigma^2}{\mu_0 c}\left(\frac{q}{4\pi\epsilon_0\varsigma}\right)^2\left(\frac{\sigma_z^2}{R_w c^2}\right)^2\int\frac{d\Omega}{\omega_\vartheta^2}\int_0^\infty\omega^4\exp\left(-\frac{\omega^2}{\omega_\vartheta^2}\right)d\omega \\ &= \frac{3\sqrt{\pi}}{4}\,\frac{1}{\mu_0 c}\left(\frac{q}{4\pi\epsilon_0}\right)^2\left(\frac{\sigma_z^2}{R_w c^2}\right)^2\left(\frac{2\gamma^2 c}{\sigma_z}\right)^3\int_0^\infty\frac{2\pi\vartheta d\vartheta}{\left(1+\gamma^2\vartheta^2\right)^3} \\ &= \frac{3}{16\sqrt{\pi}}\,\frac{q^2\gamma^4}{\epsilon_0}\,\frac{\sigma_z}{R_w^2}\ . \end{aligned} \tag{2.20}$$

Numerically $3/(16\sqrt{\pi}) = 0.1058$, which does not agree with $\sqrt{\pi}/(6\pi) = 0.0940$, which is the corresponding coefficient of U_1. (This agreement is at least as good as some of the other results, but it should be checked, since only back and forth Fourier transformation has been performed and I expected better agreement.)

Since the intended purpose of the undulator is to produce X-rays, it is important to estimate typical wavelengths:

$$\lambda_0 = 2\pi\,\frac{c}{\omega_0} = \frac{\pi\,\sigma_z}{\gamma^2}\ . \tag{2.21}$$

Note, with σ_z given by Eq. (2.8), and λ_γ given by Eq. (1.1), that $\lambda_0 = \lambda_\gamma$. Of course this is more than a coincidence, but it is not tautological. λ_γ is a characteristic of the radiation from a full periodic structure, while λ_0 is characteristic of the radiation from one half-wiggle.† With the wiggler field shape being treated as a sinuisoid with wavelength equal

† In principle the length of half-wiggle sections of a wiggler could be very short compared to the wiggler period. Then we would have $\lambda_0 << \lambda_\gamma$, and high order diffraction maxima would become significant. The same would be true if the wiggler field shape were more nearly an ideal square wave.

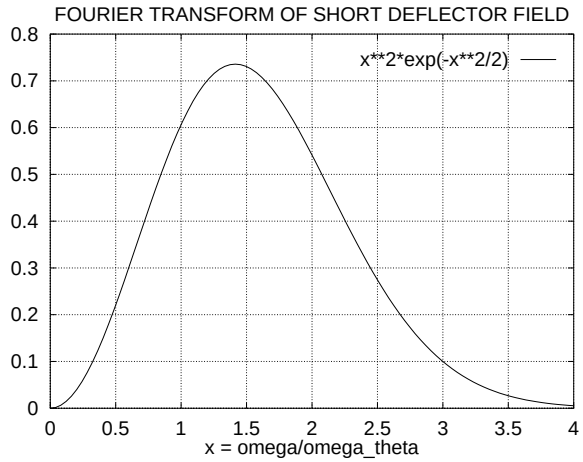

Figure 2.3: Fourier transform of deflecting force due to a short Gaussian deflecting element. For $\vartheta = 0$ the horizontal axis is ω in units of ω_0. For $\vartheta \neq 0$ the shape is the same provided the horizontal axis is taken to be ω in units of ω_ϑ. The energy spectrum is proportional to the square of this function. Thinking of the radiation as made up of photons, these are the photons one has "to work with". As in an optical diffraction grating, the most interference effects can do to "concentrate" the energy present is by transforming it into the form of photons centered on one or more diffraction maxima.

to the wiggler period the (near) equality of λ_0 and λ_γ is assured. The importance of their having comparable values is that there is a substantial flux of photons having wavelengths capable of constructive interference with the radiation from all the other "poles" of the wiggler. From Fig. 2.3 one sees that there is appreciable amplitude up to two or three times ω_0. Because positive and negative wiggles are being treated independently, the first order diffraction maximum occurs at $\omega = 2\omega_0$. One now sees from the figure that the amplitudes of higher order diffraction maxima will be negligible.

λ_0 has the remarkable feature of being independent of R_w, the central deflecting radius of curvature. The first person to emphasize the experimental significance of this feature was apparently R. Coisson,[4] Unlike regular arc radiation, the short magnet spectrum extends to high energies even when the deflection angle is small. The theory has been amply corroborated at CERN, as part of diagnostics of the SPS, a 400 GeV proton accelerator; R. Bossart et. al,[5]

That the wakefield undulator produces high energy X-rays has been established. It remains to be seen how monochromatization occurs and whether sufficiently great intensities can be obtained to make a useful device.

3. Coherence From Multiple Deflections

A single electron is subject to $2N_w$ undulator pulses, of alternating polarity, with each pulse having r.m.s. (retarded time) duration σ_z/c. All radiated beams are centered on the same straight line. Consider a component of the radiation having wavelength λ and direction ϑ. A reference wavefront is defined to be the plane passing through the emission point and perpendicular the photon's direction. As the electron advances the distance $\lambda_w/2$ from one deflection to the next, its travel time is $(\lambda_w/2)/\overline{v}$. Meanwhile the reference wavefront has traveled a distance $(\lambda_w/2)(c/\overline{v})$. Referring to Fig. 3.1, consider another wavefront which is parallel to the original wavefront, but passes through the new emission point. The distance of this wavefront from the first emitter is $(\lambda_w/2)\cos\vartheta \approx (\lambda_w/2)(1-\vartheta^2/2$. The phase difference between these two wavefronts is

$$\Delta\phi\,(\vartheta) = 2\pi\,\frac{\lambda_w}{2}\,\frac{c/\overline{v}-1+\vartheta^2/2}{\lambda} = \pi\,\frac{\lambda_w}{\lambda}\left(\frac{1}{2\gamma^2}+\frac{\Delta\Theta^2}{4}+\frac{\vartheta^2}{2}\right)\ . \tag{3.1}$$

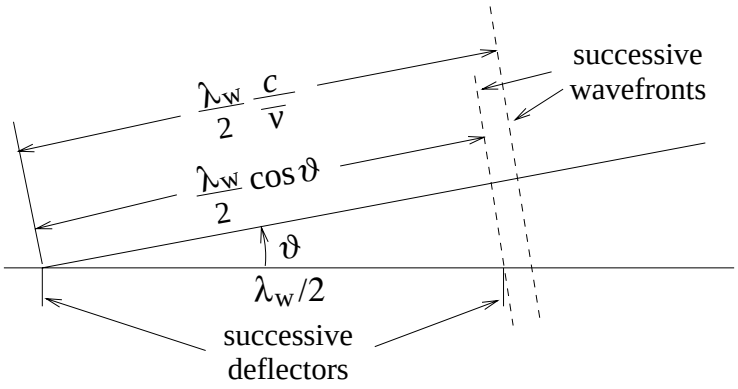

Figure 3.1: Geometry illustrating the condition for interference maximums observed at vertical angle ϑ.

In a "Fraunhofer approximation", in which all emission at angle ϑ is "focused at infinity" the condition for the two waves to interfere constructively is that this phase shift be $\pi\,n$ where n is any odd positive integer. That is

$$\lambda_n\,(\vartheta) = \frac{\lambda_w}{n}\left(\frac{1}{2\gamma^2}+\frac{\Delta\Theta^2}{4}+\frac{\vartheta^2}{2}\right)\ , \quad \text{or} \quad \omega_n\,(\vartheta) = \frac{2\pi\,c\,n}{\lambda_w}\left(\frac{1}{2\gamma^2}+\frac{\Delta\Theta^2}{4}+\frac{\vartheta^2}{2}\right)^{-1}\ . \tag{3.2}$$

(Values with $\vartheta = 0,\ n = 1$ have previously been denoted λ_γ and ω_γ.) According to Eq. (2.13) the total energy radiated is proportional to $\Delta\Theta^2$. We see therefore, that there

is a trade-off between intensity and wavelength shift. It is this trade-off that has often pushed beamline designs from the undulator regime into the wiggler regime.

Due to betatron oscillation, the electron's angle θ_e, relative to the central axis, will not be zero, and there is a longer effective deflector spacing, obtained by $\lambda_w \to \lambda_w / \cos\theta_e$. But, because λ_w appears as a multiplicative factor in Eq. (3.2), this is a relatively insignificant effect.† For the same reason, though the term $\Delta\Theta^2/4$ gives an (undesirable) shift to longer wavelenth of $\lambda_n(\vartheta)$, it does not cause the (typically more serious) broadening‡ caused by the $\vartheta^2/2$ term (due to finite out-of-plane acceptance of the detector.) To avoid unacceptably large shift of interference maxima it will be necessary to check a condition such as

$$\Delta\Theta \overset{\sim}{<} \frac{1}{2\gamma} \ , \tag{3.3}$$

that limits the shift to the 10% level. This will be referred to as the "ideal undulator condition". It will be comfortably satisfied for any feasible level of microwave power.

In the limit $\Delta\Theta << 1$, from Eq. (3.2), the relation between fundamental frequency and production angle is

$$\omega_\gamma(\vartheta) = \frac{\omega_0}{1+\gamma^2\vartheta^2} \ , \tag{3.4}$$

This function is plotted in Fig. 3.2. Note, from Eq. (2.17), that the angular dependencies of ω_γ (diffraction maximum of the multisource pattern) and ω_ϑ (frequency width of the single source pattern) are the same (in the $\Delta\Theta = 0$ limit.) This causes the diffaction maximum to retain its same position relative to the the single source spectrum, independent of production angle.

To calculate the multiple source interference pattern we sum the amplitudes from $2N_w$ deflectors, using the phasor construction of Fig. 3.3. For the special case, $\vartheta = 0$, $\Delta\Theta = 0$, using Eq. (3.5), the phase slip per deflection, expressed in terms of ω, is given by

$$\Delta\phi(0) = \frac{1}{2}\frac{\lambda_w}{\sigma_z}\frac{\omega}{\omega_0} = \pi\frac{\omega}{\omega_0} \ , \tag{3.5}$$

† Of course, the angular divergence of the radiated photon beam cannot be less than the angular divergence of the electron beam. This would only be possible if the radiation from different electrons were coherent; this would be true only at absurdly long wavelengths, as in a free electron laser.

‡ Because there is a functional relation between production angle and wavelength, the beam brilliance could, in principle, be infinite, in spite of the "Doppler" spread. In principle, the detection apparatus could be designed to take advantage of this. For example, if the beam is shone directly on a crystal, without having passed through a monochromator of other filter, the program analysing the diffraction pattern could exploit its full knowledge of the correlation. In practice the detection apparatus will usually sum over a finite range of ϑ, which will reduce the brilliance.

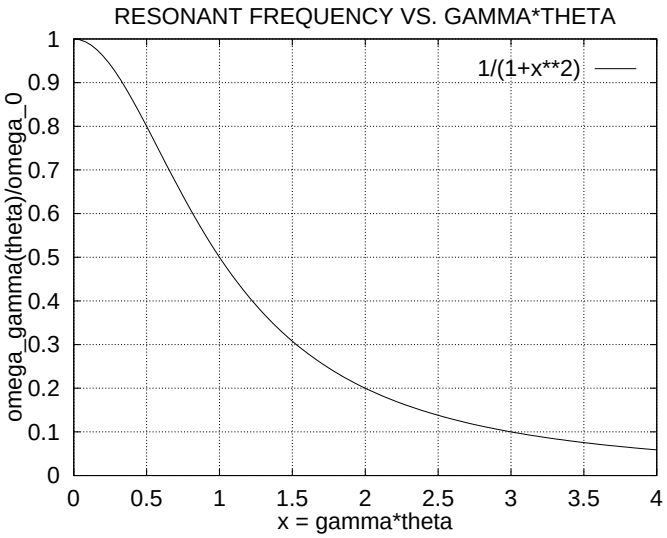

Figure 3.2: Fundamental frequency $\omega_1(\vartheta) \equiv \omega_\gamma(\vartheta)$ plotted as a function of production angle ϑ. Some people refer to this as a "Doppler shift", based on an analysis in which the radiation is first evaluated in the rest frame of the electron, and then transformed to the laboratory frame.

where the ratio λ_w/σ_z has been obtained using the caption to Fig. 2.2. $\Delta\phi(0)$ has been expressed in this form for convenient comparison with Fig. 2.3, in which the horizontal axis is ω in units of ω_0. But it is more efficient to perform the phasor calculation in terms of $\Delta\phi$ than in terms of ω, so that the dependence on ϑ and $\Delta\Theta$ will be included implicitly. The calculation indicated by Fig. 3.3 obtains a multiplicative "grating function"

$$G\left(2N_w, \Delta\phi\right) = \frac{\sin^2 \frac{2N_w \Delta\phi}{2}}{\sin^2 \frac{\Delta\phi}{2}} \ . \tag{3.6}$$

For $2N_w = 20$, the function $G(20, \Delta\phi)\widetilde{\mathbf{E}}_x^2(\omega, 0)$, with $\Delta\phi$ given by Eq. (3.5), is plotted in Fig. 3.4 with, as yet, arbitrary units for the vertical scale. A logarithmic scale is used, to make the second harmonic peak visible, and show that it is negligible. (The replacement of sinusoid by Gaussian has caused this peak to be underestimated, but not by a large factor.) No line spreading due to finite vertical acceptance is included in this spectrum.

The spectrum (for $K << 1$ and integrated over production angle) is shown in Fig. 3.5, from Jackson. Defining $\nu = \omega_\gamma(\vartheta)/\omega_0$, and P to be the total beam power, Jackson gives the frequency spectrum to be

$$\frac{dP}{d\nu} = 3P\left(\nu - 2\nu^2 + 2\nu^3\right) \ , \quad \text{for} \quad 0 < \nu < 1 \ . \tag{3.7}$$

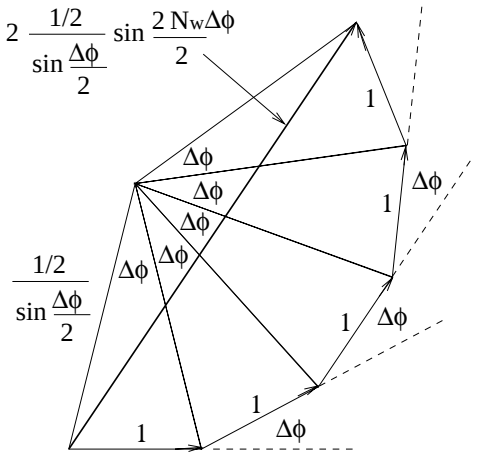

Figure 3.3: Phasor diagram with $2N_w$ arrows to calculate the coherent sum of waves from $2N_w$ sources, or N_w undulator periods. The factor multiplying the amplitude per source is $\sin(2N_w\Delta\phi/2)/\sin(\Delta\phi/2)$, where $\Delta\phi$ is the phase advance per half period of the undulator. The directions of alternate phasors are reversed to account for the half period phase shift.

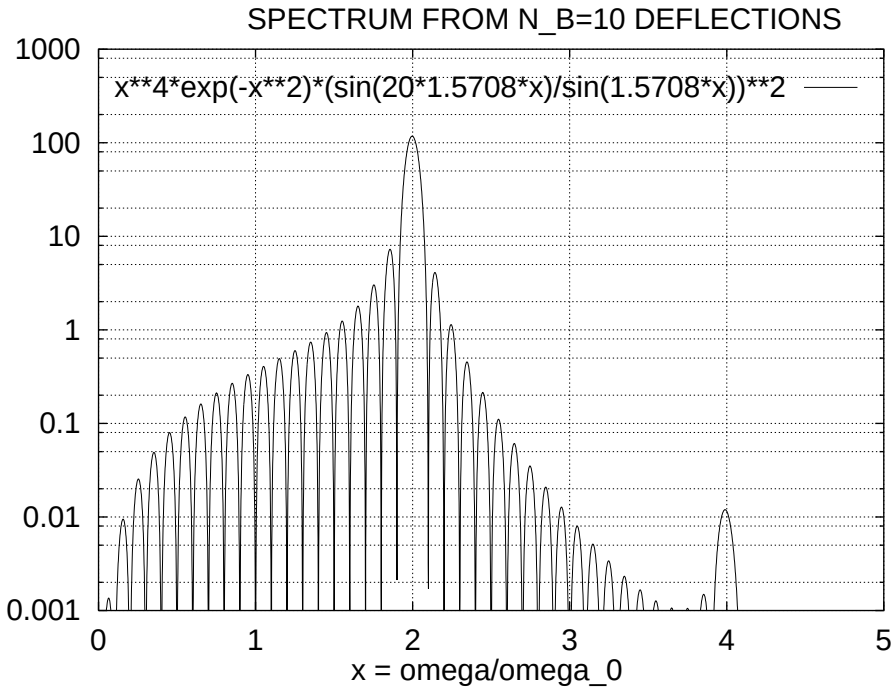

Figure 3.4: Energy spectrum for $N_w/2 = 10$ undulator periods, with numerical values assumed in the text and with $\vartheta = \Delta\Theta = 0$.

(Of course the discontinuous drop to zero at $\nu = 1$ is valid only as $N_w \to \infty$. For finite N_w the spectrum falls continuously over a range $\approx 1/N_w$.) Relative to (3.7), the number spectrum acquires a factor of ν and is hence roughly uniform over the range $0 < \nu < 1$.

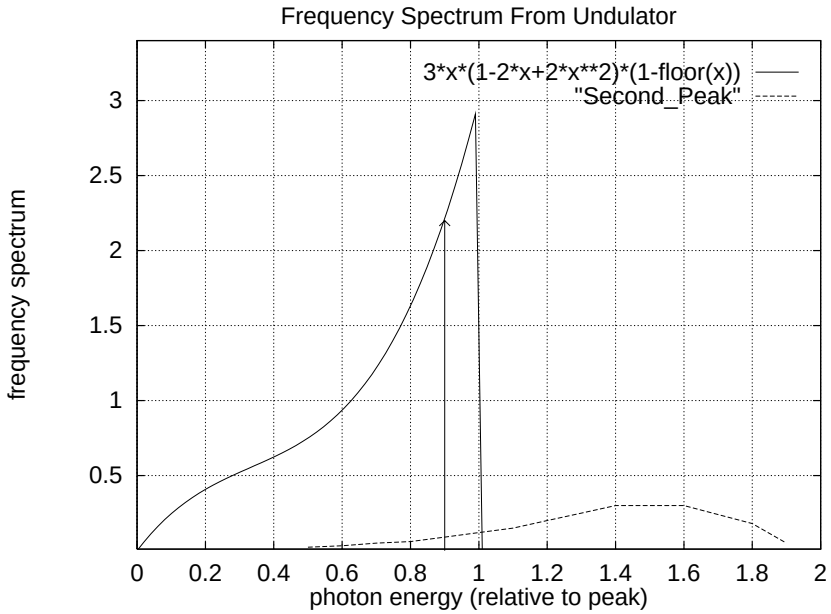

Figure 3.5: Undulator frequency spectrum plots copied (combined and somewhat garbled) from figures in Jackson, *Classical Electrodynamics*. The spectra plotted assume the production angle has been integrated over. The $K = 0$ functional form can be read from the key in the upper right corner. Preceeding the apparatus by a collimator that stops angles greater than one third of the cone angle of the radiation, would allow only the narrow energy band above the arrow to be transmitted. The second interference maximum is shown corresponding to $K = 0.5$.

But, for purposes of accounting, we will count photons as if they all had the full energy (certainly an undercount of actual photons, almost certainly a serious overcount of useful photons) and restore appropriate angle and energy dependencies later.

Because of the correlation between energy and angle, the actual number of useful photons depends on the detailed experimental setup. Conventionally the "useful" fractional energy range is taken to be $\Delta\nu = 10^{-3}$. From Eq. (3.7), the fractional power in the range $1 - \Delta\nu < \nu < 1$ works out to be

$$\frac{\Delta P}{P} = 3\Delta\nu \ . \tag{3.8}$$

Only three parts in one thousand of the pure undulator spectrum falls within the nominal energy bandwidth and the flux is therefore reduced by a factor of 330. The narrowing can be performed using a monochromator but, because of the correlation between energy and angle, it is sensible to first narrow the energy spectrum by collimating the beam to pick

out a central circular cone. Using Eq. (3.4), the corresponding solid angle factor is

$$\pi\vartheta^2 = \pi\,\frac{\Delta\nu}{\gamma^2}\ . \tag{3.9}$$

In reckoning the brilliance, which includes a factor, "per unit solid angle", a factor of $1/\Delta\nu$ is recovered. In this paper I assume that the experimenters are clever enough to extricate this correlation from their X-ray defraction results, so I will not derate the flux by this factor of 330, and I will not re-inflate the brilliance by the factor of order 10^3.

4. Radiation Intensity From Microwave Undulator

Certain intensity limits are inherent to the ideal operation of an undulator. Based on Eq. (3.3), the maximum deflection angle satisfies $\Delta\Theta < 1/(2\gamma) = 0.05\,\mathrm{mr}$, a fairly modest angle. But, since this deflection occurs over a short length, the local curvature may be substantial. The maximum total energy radiated, as a fraction of radiation per turn, can be related to $\Delta\Theta$ using Eq. (2.13);

$$\frac{U_{\rm tot}}{U_0} = \frac{2N_w}{\pi^{3/2}}\,\frac{R_0}{\sigma_z}\,\Delta\Theta^2 \quad \left(\overset{\text{e.g.}}{=} \frac{2N_w}{2\pi^{3/2}}\,\frac{90}{0.01}\times\frac{10^{-8}}{4} \approx 0.4\times10^{-5}\ (2N_w)\right)\ . \tag{4.1}$$

What makes the undulator promising, in spite of this relatively low upper limit, is the "short magnet enhancement"† that shifts all the radiated energy into a narrow high energy band. As well as the factor $2N_w$ explicitly exibited in Eq. (4.1), the beam brilliance acquires another factor $2N_w$ from the diffractive line narrowing. It seems therefore, that one need not be unduly discouraged concerning the intensity limit that follows from condition (3.3).

For the microwave undulator the maximum achievable deflection is determined by the maximum power P propagating along the waveguide. For propagation in the TE_{10} mode (which is the propagating mode with lowest cut-off frequency) the power is given by[6]

$$P = \frac{|E_{\max}|^2}{Z_0}\,\frac{ab}{2}\,\sqrt{1-\left(\frac{\lambda_{\rm rf}}{2a}\right)^2} \tag{4.2}$$

† It is this short magnet enhancement that enables the CERN proton ring diagnostics, referred to previously. In their case (because they have protons) the rate of *visible* photons is enhanced by some 23 orders of magnitude (according to Coisson.) This gigantic enhancement is possible only because of the large proton to electron mass ratio. For an electron ring like CESR, since the critical energy u_c is already in the few keV range, the enhancement is enormously less; the energy radiated per unit energy for $u = 4u_c$ is roughly ten times less than for $u = u_c$, so the number of photons radiated per unit energy falls by about 40 over the same range.

where $Z_0 = \sqrt{\mu_0/\epsilon_0} = 377\,\text{ohms}$, $E_{\max}$ is the maximum electic field, and a and b are waveguide dimensions. The wave can be represented as the sum of two waves, directed at angles θ on one or other side the axis, where

$$\cos\theta = \sqrt{1 - \left(\frac{\lambda_{\rm rf}}{2a}\right)^2} \ . \tag{4.3}$$

In this mode the cut-off wavelength is $2a$. Since we favor waves propagating more or less parallel to the waveguide axis, $\theta << \pi$, we will have $\lambda_{\rm rf} << 2a$, so the square root factor in Eq. (4.2) will be approximately 1. For example, $a = \lambda_{\rm rf}$ will yield $\cos\theta = 0.866$, $\theta = 30°$.

The total deflection per half period also depends on the particular waveguide propagation mode but, for simplicity, let us consider only the case of propagation exactly parallel to the waveguide axis. (As a matter of fact, there is no such mode, but short wavelength modes can propagate approximately parallel to the guide.) The motion of a charged particle in an electromagnetic wave is analyzed in Appendix A. According to Eq. (A.19), the maximum deflection angle is given by

$$\Delta\Theta = \frac{dx}{d\Phi}\Big|_{\max} \frac{d\Phi}{dz} \approx \frac{2\omega_{\rm rf}}{c} \frac{e\,E_{\max}}{\mathcal{L}\,m\,\omega_{\rm rf}^2} = \frac{1}{\gamma}\,\frac{\lambda_{\rm rf}}{2\pi}\,\frac{E_{\max}}{mc^2/e} \quad \left(\approx \frac{1}{\gamma}\,\frac{\lambda_{\rm rf}}{2\pi}\,\frac{E_{\max}\,(\text{MV/m})}{0.511\,\text{MV}}\right) \ . \tag{4.4}$$

Since RF field gradients as high as 100 MV/m are physically achievable (if only for brief pulses) it is possible to briefly achieve deflections $\Delta\Theta \sim 1/\gamma$, which is as large as is consistent with ideal undulator operation.

But, for CW operation, it is more meaningful to relate $\Delta\Theta$ to microwave power. To avoid the extravagance of supporting CW power P, it is sensible to establish a standing wave pattern† in a (long) waveguide resonator of length L_w. There is a possible advantage to making this tube circular, so that arbitrarily-polarized, linear, circular, etc., waves could be established. But, to simplify the discussion, we are considering only a rectangular tube of width a and height b, carrying the TE_{10} mode. Using a superconducting RF cavity may also be attractive, but the following numerical estimate will assume the waveguide is made of room temperature copper. This choice would be especially convenient because the waveguide could be continuous through the magnets making up the beam line, and hence could be made almost arbitrarily long without disrupting the lattice optics seriously.

† A ring resonator configuration could support only forward-traveling waves, with similar power considerations.

The power $P(z)$ of a wave propagating in the $+z$ direction in a waveguide satisfies

$$-\frac{dP}{dz} = 2\alpha P \ , \tag{4.5}$$

which means that $2\alpha P$ can be interpreted as the power per meter flowing into the walls. Neglecting end losses, the external power $P_{\text{ext.}}$ required to maintain a standing wave (sum of equal but opposite traveling waves) in a guide of length L_w therefore satisfies

$$\frac{P_{\text{ext.}}}{P} = 4\alpha L_w \ . \tag{4.6}$$

In the TE_{10} mode α (the inverse of the distance over which E and H fall by $1/e$) is given by

$$\alpha = \frac{1}{b}\sqrt{\frac{\pi}{Z_0 \sigma \lambda_{\text{rf}}}}\,\frac{1+\frac{2b}{a}\left(\frac{\lambda_{\text{rf}}}{2a}\right)^2}{\cos\theta}, \tag{4.7}$$

where the numerical values appropriate for room temperature copper are $\sigma_{\text{cu}} = 4.0 \times 10^7/\text{ohm/m}$ and $\pi/(Z_0\sigma) = \pi/(376.7 \times 4.0 \times 10^7) = 2.08 \times 10^{-10}\,\text{m}$. We obtain, in this case, using $\lambda_{\text{rf}} = a = 0.04\,\text{m}$, $b = 0.02\,\text{m}$,

$$\begin{aligned}\frac{P_{\text{ext.}}}{P} &= \frac{4L_w}{b}\sqrt{\frac{2.08\times10^{-10}\,(m)}{\lambda_{\text{rf}}\,(m)}}\,\frac{1+\frac{2b}{a}\left(\frac{\lambda_{\text{rf}}}{2a}\right)^2}{\cos\theta} \\ &\left(\overset{\text{e.g.}}{=} \frac{4L_w\,(m)}{0.02\,(m)}\sqrt{\frac{2.08\times10^{-10}}{0.04}}\,\frac{1.25}{0.866} = \frac{L_w\,(\text{m})}{48.1\ (\text{m})}\ .\right)\end{aligned} \tag{4.8}$$

Aside concerning cryogenic waveguide. I am grateful to Maury Tigner for making the following, probably decisive, clarification plus suggestion. It has been implicit in the discussion that a major advantage of the microwave undulator is that it can pass through magnetic lattice elements (quadrupoles.) This permits L_w to be long without having appreciable impact on the lattice optics. Though the power estimates have assumed room temperature copper waveguide, it would seem to be both natural and technically possible to pass cryogenic waveguide through the magnetic elements. Tigner's clarification was that strong magnetic field ruins the Q factor of superconducting resonators. This rules out, or greatly complicates any superconducting RF design. His suggestion was to consider using ultrapure copper waveguide run at liquid nitrogen temperature, where its resistance is close to ten times less than at room temperature. This reduces α, and hence P_{ext} at fixed P, by a factor close to three. Since the power extraction efficiency will be less than the

Kelvin factor 80/300 by other refrigerator inefficiency, there would be a net power penalty for this cryogenic approach. But (because the duty factor is likely to be fairly small) the power bill is not likely to be a decisive issue, and other technical problems would be greatly simplified.

Aside concerning waveguide dimensions. The waveguide dimensions have been taken to be $a = 0.04\,\mathrm{m}$, $b = 0.02\,\mathrm{m}$. At the nominal RF wavelength $\lambda_{\mathrm{rf}} = 0.04\,\mathrm{m}$, this waveguide will support only an electric field that is perpendicular to the broad side. This would invalidate the claim that the X-ray polarization can be readily switched. Since doubling b increases the surface area by only a factor $16/12 = 1.33$, this would cause only a modest increase in power (or reduction in brilliance.) Another claimed feature of the microwave undulator is that the X-ray energy can be changed dynamically. The most important use for this feature is likely to entail only tiny energy changes from just below to just above an absorbtion edge. Such small changes are likely to be fairly easy. Changes over large ranges are far more problematical.

Returning to the estimate of radiated power, using Eq. (4.2) and Eq. (4.8), $\Delta\Theta^2$ can be expressed as

$$\Delta\Theta^2 \approx \frac{1}{\gamma^2}\,\frac{1}{\sqrt{1-\left(\frac{\lambda_{\mathrm{rf}}}{2a}\right)^2}}\,\frac{1}{2\pi^2}\,\frac{\lambda_{\mathrm{rf}}^2}{ab}\,\frac{P}{\left(mc^2/e\right)^2/Z_0} \quad \left(\approx \frac{1}{\gamma^2}\,\frac{1}{2\pi^2}\,\frac{\lambda_{\mathrm{rf}}^2}{ab}\,\frac{P_{\mathrm{ext.}}\,(MW)}{693.1\,\mathrm{MW}}\,\frac{48.1\ (\mathrm{m})}{L_w\,(\mathrm{m})}\ .\right) \tag{4.9}$$

For an external power level $P_{\mathrm{ext.}} \approx 1\,\mathrm{MW}$, this factor will be about $10^{-3}/\gamma^2$. In this case the X-ray flux per unit length will be less than from a $K = 1$ (the largest value consistent with "ideal" behavior) undulator by a factor of one thousand. For a superconducting waveguide this factor could be much closer to one. In absolute terms, from Eq. (4.1), the total radiated power is given by

$$\frac{U_{\mathrm{tot}}}{U_0} = \frac{2N_w}{2\pi^{7/2}}\,\frac{R_0}{\sigma_z}\,\frac{1}{\gamma^2}\,\frac{1}{\sqrt{1-\left(\frac{\lambda_{\mathrm{rf}}}{2a}\right)^2}}\,\frac{\lambda_{\mathrm{rf}}^2}{ab}\,\frac{P}{\left(mc^2/e\right)^2/Z_0}\ . \tag{4.10}$$

The power radiated from an undulator of length $L_w = N_w\lambda_w$ can be estimated by recalling that the pure antiparallel assumption leads to $\lambda_w \approx 2\lambda_{\mathrm{rf}}$ and $\sigma_z \approx \lambda_{\mathrm{rf}}/(4\pi)$. With these approximations we obtain for U_{tot}, the power radiated by a single electron,

$$\frac{U_{\mathrm{tot}}}{U_0} \approx \frac{4}{\pi^{5/2}}\,\frac{L_w\,R_0}{ab}\,\frac{1}{\gamma^2}\,\frac{P_{\mathrm{ext.}}\,(MW)}{693.1\,\mathrm{MW}}\,\frac{P}{P_{\mathrm{ext.}}}\ . \tag{4.11}$$

Since the final factor causes this to be independent of L_w, contrary to what one might have expected, the power of the produced X-ray beam (per unit of external microwave power) will be independent of L_w. Nevertheless, high brilliance will favor large L_w. (The formulas determining power that have been given will also become more nearly valid as L_w is increased.)

For beam current I, the number of electrons traversing the undulator per second is $I/e = 0.62 \times 10^{19}$ /A/s. Because the width of the energy spectrum is inversely proportional to the number of undulator periods N_w, and the flux is reckoned per tenth percent bandwidth, there is a sensitive dependence of "flux" $\mathcal{F}'$ on N_w. Let us assume that N_w, though large, is small enough that the fractional energy width (at fixed angle) exceeds one tenth percent. Then (to accuracy not better than a factor of two) the flux acquires a rough factor $N_w/10^3$, and the flux per tenth percent bandwidth (at all energies and angles, but with peak value $h\nu = 12.4\,\mathrm{keV}$) is given by

$$\begin{aligned}\mathcal{F}' = \frac{U_{\mathrm{tot}}}{h\nu}\,\frac{I}{e}\,\frac{N_w}{10^3} &\approx \frac{4}{\pi^{5/2}}\,\frac{L_w\,R_0}{ab}\,\frac{U_0}{h\nu}\,\frac{I}{e}\,\frac{1}{\gamma^2}\,\frac{P_{\mathrm{ext.}}\,(MW)}{693.1\,\mathrm{MW}}\,\frac{P}{P_{\mathrm{ext.}}}\,\frac{N_w}{10^3} \\ &\left(\overset{\text{e.g.}}{=} 0.229\,\frac{0.885\times10^{-4}\times5.11^4\times10^9}{0.04\times0.02\times1.24\times10^4}\,\frac{0.62\times10^{19}}{10^8\times693.1\times0.0208}\,\frac{N_w}{10^3}\right. \\ &\left.= 0.60\times10^{16}\,\frac{N_w}{10^3}\,\frac{\mathrm{photons/s}}{\mathrm{MW\text{-}A}}\;.\right)\end{aligned} \tag{4.12}$$

The power ratio estimate of Eq. (4.8) has been used. For $L_w = 10\,\mathrm{m}$, $N_w = 10/0.02$, about half of the photons will fall within the nominal 0.1% bandwidth. Taking $I = 0.1\,\mathrm{A}$, the flux† (including all angles) will be

$$\mathcal{F}'_{0.1\mathrm{A}} = 3.0\times10^{14}\,\frac{\mathrm{photons/s/0.1\%BW}}{\mathrm{MW}}\;. \tag{4.13}$$

On economic grounds a continuous power of $P_{\mathrm{ext.}} = 1\,\mathrm{MW}$ would probably be tolerable but, in practice, even "CW operation" would employ a duty factor far less than 1, so 1 MW seems like a conservative estimate for the microwave power (assuming this power level can be supported without breakdown.) Of course it would give a big improvement

† As mentioned previously, the beam power is being accounted for as if made up of full-energy photons so, to obtain the actual number distribution in angle and energy of photons, Eq. (4.13) would need to be manipulated. Without this having been done, Eq. (4.13) is not very useful for making comparisons with other X-ray sources. The symbol $\mathcal{F}'$, rather than $\mathcal{F}$, is intended to be a reminder of this unconventional usage.

to use superconducting waveguide instead of the copper that has been assumed. Ignoring the dependence of energy on angle, the X-ray beam power corresponding to Eq. (4.13) is $\mathcal{P} \approx 2 \times 3 \times 10^{14} \times 1.24 \times 10^4 \approx 10^{19}\,\mathrm{eV/s}$ at 1 MW.

For comparison purposes, Fig. 4.1 shows performance of a conventional, 5 mm gap, undulator as reported by Walker.[7] This is just a crude fit, crudely extrapolated, and it refers to operation at $E_e = 1.5\,\mathrm{GeV}$. The flux at 12.4 keV is down by about three orders of magnitude from the value given in Eq. (4.13). On the other hand, the X-ray beam power, (given in the caption to the figure) is about 10^{19} keV/s. According to these estimates, the flux from the microwave undulator is three orders of magnitude greater even though the beam power is three orders of magnitude less.

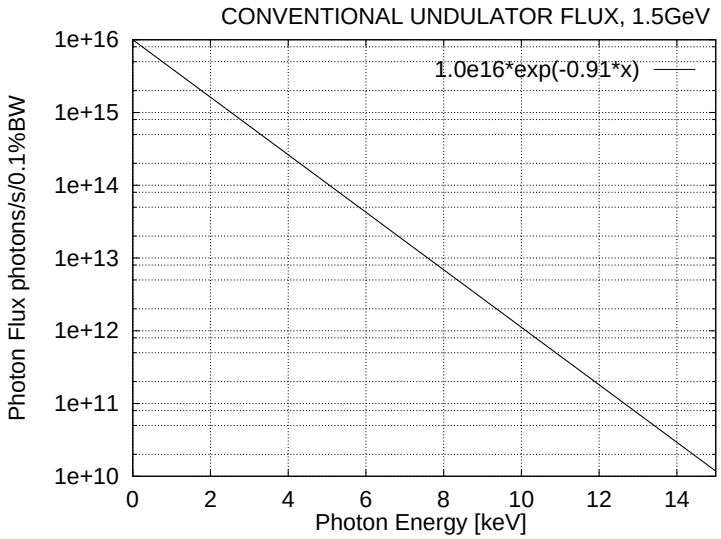

Figure 4.1: Fit to flux from conventional wiggler[7] operating with 5 mm gap and beam energy $E = 1.5\,\mathrm{GeV}$. The straight line crudely approximates 8 diffraction maxima in the range up to 10 keV and extrapolates to 15 keV. Integrating over the distribution given in the key yields a total beam power $\mathcal{P} \approx 10^{19}$ keV/s.

5. Accelerator Physics Considerations

To complete the determination of intensity, brilliance, distribution functions and other parameters of the produced beam, it is necessary to address accelerator physics practicalities. For a start, because the radiated power is so weak, it seems safe to neglect degradation of the electron beam caused by the microwave (except due to peripheral effects such as requiring too small vacuum tube dimensions or causing vacuum degradation due to microwave heating.)

One can envisage a waveguide undulator passing right through some of the magnets making up the accelerator lattice. An example of the lattice optics of a sequence of six minimum emittance cells, is shown in Fig. 5.1. An waveguide undulator as long as 15 meters could be placed within the zero-dispersion central straight section. (The purpose of having zero dispersion is to minimize the influence of the undulator on the circulating beam.)

It is implicitly assumed in most discussions of synchrotron radiation (including this one) that the bend plane is horizontal and is designated as the x plane; the dominant field component is then E_x. (For the same reason) practical electron beams are usually ribbon-shaped, with transverse sigmas related by $\sigma_y << \sigma_x$. Because of this, it could turn out that vertical deflections would give superior performance for some purposes I leave this as an open question, but continue to assume implicitly that the bend plane is horizontal.

For any one electron, it has been argued that the spectrum is rather insensitive to the particle's slope. In this sense the accelerator optics at the undulator is unimportant. It is true however, that the spike visible in Fig. 3.4 is as sharp as it is because a restricted range of angle ϑ has been assumed. Commonly one will wish to limit line broadening by exploiting the correlation between production angle and wavelength by limiting ϑ. It therefore seems sensible to perform collimation at a large distance where the transverse position is dominated by production angle rather than production position. A collimator at such a position will limit the ϑ range. Such an aperture will only be effective if the spread of electron angles is small compared to $1/\gamma$.

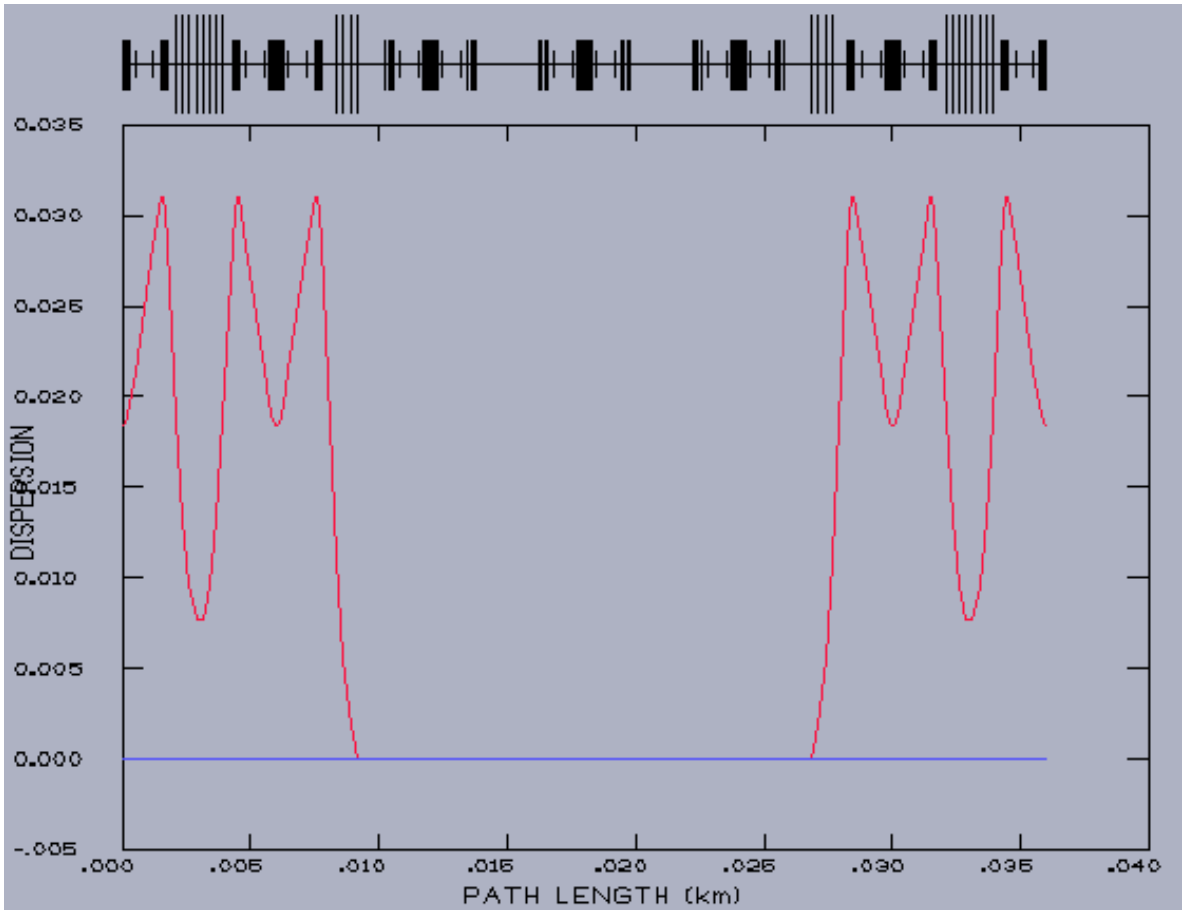

Figure 5.1: Six consecutive minimum emittance cells, with the second and fifth cells modified to provide zero dispersion in the third and fourth cells. Bending magnets, quadrupoles, and sextpoles are indicated by long medium and short hatch marks in the schematic above the graph.

The spatial and angular width parameters that influence the brilliance are contained in the product

$$\sigma_{\gamma,x}\sigma_{\gamma,x'}\sigma_{\gamma,y}\sigma_{\gamma,y'} = \sqrt{\beta_x\epsilon_x}\,\sqrt{\frac{\epsilon_x}{\beta_x}+\frac{f}{\gamma^2}}\,\sqrt{\beta_y\epsilon_y}\,\sqrt{\frac{\epsilon_y}{\beta_y}+\frac{f}{\gamma^2}} \approx \sqrt{\beta_x\epsilon_x}\,\sqrt{\beta_y\epsilon_y}\,\frac{f}{\gamma^2} \qquad (5.1)$$

where f is a dimensionless ω-dependent numerical factor, obtainable from Eq. (2.19). For $f \approx 0.5$, a typical value, $f/\gamma^2 \approx 0.5\times10^{-8}$ m. In the last step a "low emittance" lattice has been assumed, which amounts to neglecting electron angular spreads relative to photon angular spreads. This approximation is not very bad even for a machine with gigantic emittances, such as CESR.

Using Eq. (5.1) is tantamount to assuming that the detection apparatus accepts and utilizes the full photon cone angle. In practice, the cone angle would be reduced by

collimation. According to Eq. (3.9), this would reduce the solid angle (and hence photon rate) and energy spread more or less proportionally. The brilliance, a ratio of photon rate to solid angle, would therefore tend to be more or less independent of collimation angle, except that, by convention, one is to count only photons in the tenth percent bandwidth. Because Eq. (5.1) has already incorporated the undulator-effect reduction of fractional energy spread to be of the order of $1/N_w$, this requirement has already been built into Eq. (5.1). As a result there is really a unique angular collimation compatible with this formula—that which limits the fractional energy spread to $\Delta\nu = 10^{-3}$. Since this formalism is almost certainly different from that employed by others, I will use $\mathcal{B}'$ as its symbol. $\mathcal{B}'$ is obtained by combining Eqs. (4.12) and (5.1);

$$\mathcal{B}' = \frac{\mathcal{F}'}{\pi^2\sigma_{\gamma,x}\sigma_{\gamma,x'}\sigma_{\gamma,y}\sigma_{\gamma,y'}} = \frac{1}{\pi^2}\,\frac{4}{\pi^{5/2}}\,\frac{L_w\,R_0}{ab}\,\frac{U_0}{h\nu}\,\frac{I}{e}\,\frac{P_{\text{ext.}}\,(MW)}{693.1\,\text{MW}}\,\frac{P}{P_{\text{ext.}}}\,\frac{N_w}{10^3}\,\frac{1/f}{\sqrt{\beta_x\epsilon_x}\,\sqrt{\beta_y\epsilon_y}} \tag{5.2}$$

From here on $\mathcal{B}'$ will not be distinguished from brilliance $\mathcal{B}$. As has been emphasized repeatedly, since "all" the energy is concentrated in the main peak, the total power of the beam is trivially small.

There are too many uncertain factors to give a definitive numerical value to $\mathcal{B}$. The main factors multiplying the flux $\mathcal{F}'$ to give brilliance $\mathcal{B}$, are

- $1/\pi^2 \approx 10^{-1}$, a factor that accounts for the fact that the bunch σ's are one-sided measures.
- $\gamma^2 \overset{\text{e.g.}}{=} 10^8$. As mentioned below Eq. (3.9), since the flux has not been de-rated to account for the angular spread, the brilliance must not be re-inflated to account for an angular aperture much less than $1/\gamma$.
- $(f\sqrt{\beta_x\beta_y})^{-1} \overset{\text{e.g.}}{=} 1/\text{m}$, because $f \approx 0.5$ and $\sqrt{\beta_x\beta_y} \approx 2\,\text{m}$.‡
- $1/\sqrt{\epsilon_x\epsilon_y} = 10^{10}\,(\text{m-rad})^{-1}$ for an exceedingly low, but probably achievable emittance, some 4 times greater (i.e. smaller emittance) than the corresponding product at ESRF or APS.
- $10^{-12}\,(\frac{\text{m}}{\text{mm}})^2\,(\frac{\text{r}}{\text{mr}})^2$ because $\mathcal{B}$ is conventionally quoted in terms of millimeters and milliradians, rather than meters and radians.

‡ There is "headroom" for increasing $\mathcal{B}$ by decreasing either or both of β_x and β_y. Furthermore, since the waveguide can pass through the center of focusing magnets, it may be practical to keep β_x and β_y small along the length of even a long undulator.

Combining these values with the flux value given in Eq. (4.13) for a 10 m undulator yields

$$\mathcal{B}_{0.1\mathrm{A}} = 3 \times 10^{19} \, \frac{\text{photons/s/0.1\%BW/mm}^2\text{/mr}^2}{\text{MW}} \; . \tag{5.3}$$

For quantitative comparison with the brilliance achieved or advertised by other storage rings, one should be sure the assumptions going into the definition of brilliance are consistent. Various factors have been ignored, some making Eq. (5.3) too pessimistic (e.g. the factor 3 in Eq. (3.8)) others too optimistic (e.g. the treatment of the collimator, ignoring the elliptical shape of the beams, and oversimplifying the shape of the upper end of the undulator energy spectrum.) These uncertainties cause Eq. (5.3) to be little better than an order-of-magnitude estimate.

According to Suller, one of the magnetic undulators at ESRF, operating at 6 GeV.[8] produces brilliance 1.6×10^{19} photons/s/0.1%BW/mm^2/mr^2 at $h\nu = 7.4$ keV; this would be reduced by roughly a factor of ten in extrapolating to 12.4 keV. These numbers correspond to emittances $\epsilon_x = 4 \times 10^{-9}$ m and $\epsilon_y = 4 \times 10^{-11}$ m. The advertised brilliance at $h\nu =$ 12.4 keV, for an undulator in "Protein Crystallography Beamline" of SLS (The Swiss Light Source) is $\mathcal{B}_{0.4\mathrm{A}} = 0.5 \times 10^{19}$photons/s/0.1%BW/mm^2/mr^2. This line will be known as the "Protein Crystallography Beamline". The undulator gap height is (planned to be) 4 mm, beam energy is 2.6 GeV(?), and $K_{\max} = 1.65$.

The brilliance increases only as $(\sqrt{\epsilon_x \epsilon_y})^{-1}$. The reason for this is that the radiation cone has been assumed to be large compared to the (elliptical) cone of electron angles. It is necessary to check that this is valid. Because low emittance storage ring designs lead to $\langle \beta_x \rangle << \langle \beta_y \rangle$ and $\epsilon_x >> \epsilon_y$ the only condition that needs to be checked is

$$\sqrt{\frac{\epsilon_x}{\beta_x}} << \frac{1}{\gamma^2} \; . \tag{5.4}$$

The same x, y asymmetry may influence the choice of waveguide dimensions. To increase X-ray intensity at fixed microwave power there is a premium on reducing the transverse waveguide dimensions. In this paper we have been using width/height $= a/b =$ 4 cm/2 cm = 2, and will continue to do this. But, in principle the waveguide height could be reduced without violating condition (5.4) or clipping the vertical tails of the beam distribution.

Another condition to be satisfied is that the spread of "searchlight angles" of the electron beam passing through the undulator (about $K/(3\gamma)$) should roughly match the

cone angle of a collimator whose purpose is to limit the spread of X-ray energies (about $\sqrt{\Delta\nu}/\gamma \approx 1/(30\gamma)$. This sets a limit $K < 0.1$. Since flux and brilliance are proportional to K^2, this consideration helps to make the brilliance from the microwave undulator (where achieving high K is difficult) competitive with the brilliance from a magnetic undulator (where achieving high K is easy.)

Reducing the horizontal emittance ϵ_x improves the X-ray beam brightness, but there is a value below which diminishing returns set in. A matching condition based on considerations similar to the previous paragraph is that the spread of "searchlight angles" of the electron beam passing through the undulator (about $K/(3\gamma)$) should not exceed the spread of electron angles (about $\sqrt{\epsilon_x/\beta_x}$.) Accepting this as a strict inequality yields

$$K < 3\gamma\sqrt{\frac{\epsilon_x}{\beta_x}}\ , \quad \text{or} \quad \epsilon_x > \frac{K^2\beta_x}{10\gamma^2}\ , \tag{5.5}$$

depending on whether the "pinch" comes from K or ϵ_x. For a long undulator β_x may have to be 10 m or greater, in which case, ϵ_x has to be K^2/γ^2 m or greater. For the Energy Recovery Linac X-ray source that has been under discussion recently, the proposed emittance is $\epsilon_x \approx 10^{-10}$. With γ being 10^4, the value of K^2 should not exceed 0.01. The flux and brilliance would be therefore be down from the $K = 1$ values by two orders of magnitude.

Appendix A.
Trajectory of electron in electromagnetic wave

This paper requires the description of charged particle orbits in a traveling electromagnetic wave and, for comparison with conventional undulators, the motion also in a periodic magnetic field. Unfortunately, though the orbits are very similar, the analysis for a periodic magnetic field cannot be subsumed into the analysis for a traveling wave, even by going to the zero frequency limit, because there is no frame of reference in which the electric field of a traveling wave vanishes. This correlates with the fact that energy transfer between particle and field is possible for a traveling wave, but not for a pure magnetic field. Such energy transfer is fundamental to the operation of free electron lasers, but is inessential to the operation of the microwave undulator being discussed in this paper.

Since the electron is highly relativistic, it is essential for relativistically valid formulas to be used. Fortunatately, exact equations of motion are known[†] for motion of a charged particle in an electromagnetic wave.

For an electromagnetic plane wave traveling in direction $\hat{\mathbf{n}}$, the electric and magnetic fields are related by

$$\mathbf{B} = \frac{1}{c}\,\hat{\mathbf{n}} \times \mathbf{E}\ , \quad \text{and} \quad \mathbf{B}\cdot\hat{\mathbf{n}} = \mathbf{E}\cdot\hat{\mathbf{n}} = 0\ . \tag{A.1}$$

For a monochromatic wave of frequency $\omega_{\rm rf}$, dependencies on both position $\mathbf{r}$ and time t can be expressed in terms of a single independent (phase) variable

$$\Phi = \omega_{\rm rf}\,(t - \hat{\mathbf{n}}\cdot\mathbf{r}/c)\ . \tag{A.2}$$

For the special case in which the wave is traveling parallel to the positive z-axis, $\Phi = \omega_{\rm rf}(t - z/c) = \omega_{\rm rf}t - kz$, where k is the photon wave number. Later, $\mathbf{r}$ will be taken to be the position of a particle with velocity $\mathbf{v} = d\mathbf{r}/dt$, and then

$$\frac{d\Phi}{dt} = \omega_{\rm rf}\,(1 - \hat{\mathbf{n}}\cdot\mathbf{v}/c)\ . \tag{A.3}$$

[†] Clemmow, P.C. and Dougherty, J.P., *Electrodynamics of Particles and Plasmas,* ascribe this theory to Kolomenskii A.A. and Lebedev A.N., *Sov. Phys. Doklady,* **7**, *745 (1963)* and *Sov. Phys. JETP,* **17**, *179 (1963).*

In effect, the variable Φ locates the particle by giving the instantaneous longitudinal projection (onto the wave normal) relative to some standard wavefront of the wave. We are primarily interested in the case in which the electron travels almost anti-parallel to the wave at almost the speed of light, $z = -|\overline{v_z}|t$. Then $\Phi = \omega_{\rm rf} t(1 + |\overline{v_z}|/c) \approx 2\omega_{\rm rf} t$.

The mechanical energy γmc^2 of an electron of velocity $\mathbf{v}$ is governed by

$$\frac{d\gamma}{dt} = \frac{e}{mc^2}\,\mathbf{E}\cdot\mathbf{v}, \tag{A.4}$$

and its equation of motion is

$$\frac{d}{dt}\left(\gamma\frac{\mathbf{v}}{c}\right) = \frac{e}{mc}\left(\mathbf{E}+\mathbf{v}\times\mathbf{B}\right) = \frac{e}{mc}\,\left(1-\hat{\mathbf{n}}\cdot\mathbf{v}/c\right)\,\mathbf{E} + \frac{e}{mc^2}\left(\mathbf{E}\cdot\mathbf{v}\right)\,\hat{\mathbf{n}}. \tag{A.5}$$

By combining these equations one shows that the quantity

$$\mathcal{L} = \gamma\,\left(1-\hat{\mathbf{n}}\cdot\mathbf{v}/c\right)\ , \tag{A.6}$$

is a constant of the motion. For exactly anti-parallel motion $\mathcal{L} \approx 2\gamma$.

We now set about changing independent variable from t to Φ in the electron's equation of motion, using primes to indicate $d/d\Phi$. Then, using Eq. $(A.3)$,

$$\mathbf{r}' = \frac{d\mathbf{r}/dt}{d\Phi/dt} = \frac{\mathbf{v}}{\omega_{\rm rf}\,\left(1-\hat{\mathbf{n}}\cdot\mathbf{v}/c\right)}\ . \tag{A.7}$$

Differentiating again yields

$$\mathbf{r}'' = \frac{1}{{\omega_{\rm rf}}^2\,\left(1-\hat{\mathbf{n}}\cdot\mathbf{v}/c\right)}\,\frac{d}{dt}\,\left(\frac{\mathbf{v}}{\left(1-\hat{\mathbf{n}}\cdot\mathbf{v}/c\right)}\right)\ . \tag{A.8}$$

Using this, after first substituting from Eq. $(A.6)$, the left hand side of Eq. $(A.5)$ can be rewritten as

$$\frac{d}{dt}\,\left(\gamma\,\mathbf{v}/c\right) = \mathcal{L}\,\frac{d}{dt}\left(\frac{\mathbf{v}/c}{1-\hat{\mathbf{n}}\cdot\mathbf{v}/c}\right) = {\omega_{\rm rf}}^2\mathcal{L}\,\left(1-\hat{\mathbf{n}}\cdot\mathbf{v}/c\right)\,\mathbf{r}''\ . \tag{A.9}$$

and, again using Eq. $(A.7)$, the right hand side is

$$\left(1-\hat{\mathbf{n}}\cdot\mathbf{v}/c\right)\,\frac{e}{m}\,\left(\mathbf{E}+\frac{\omega_{\rm rf}}{c}\mathbf{E}\cdot\mathbf{r}'\,\hat{\mathbf{n}}\right)\ . \tag{A.10}$$

These manipulations have permitted the common factor $1-\hat{\mathbf{n}}\cdot\mathbf{v}/c$ to be cancelled, and the equation of motion becomes

$$\mathbf{r}'' = \frac{e}{\mathcal{L}\,m\,{\omega_{\rm rf}}^2}\left(\mathbf{E}+\frac{\omega_{\rm rf}}{c}\mathbf{E}\cdot\mathbf{r}'\,\hat{\mathbf{n}}\right)\ . \tag{A.11}$$

This equation is exact relativistically, except for not including the radiation reaction force. We know that the only important effect of this force is the "slowing down" required by energy conservation.

For the special case in which the wave is traveling parallel to the positive z-axis, $\hat{\mathbf{n}} = \hat{\mathbf{z}}$, with electric field directed along the x-axis,

$$\mathbf{n} = (0,0,1)\,, \quad \mathbf{E} = E\,\cos\Phi\;(1,0,0)\,, \quad \mathbf{B} = \frac{E}{c}\,\cos\Phi\;(0,1,0)\,, \tag{A.12}$$

and the equations of motion are

$$x'' = \frac{e\,E}{\mathcal{L}\,m\,{\omega_{\rm rf}}^2}\,\cos\Phi, \quad y'' = 0, \quad z'' = \frac{e\,E}{c\,\mathcal{L}\,m\,{\omega_{\rm rf}}^2}\,x'\,\cos\Phi. \tag{A.13}$$

The solution to the first of these equations is

$$x' = \frac{e\,E}{\mathcal{L}\,m\,{\omega_{\rm rf}}^2}\,\sin\Phi, \quad x = -\frac{e\,E}{\mathcal{L}\,m\,{\omega_{\rm rf}}^2}\,\cos\Phi, \tag{A.14}$$

where integration constants have been dropped since we now assume the particle is, on the average, moving with no transverse drift along the z-axis. Then the third of Eqs. (A.13) becomes

$$z'' = \frac{1}{2\,c}\left(\frac{e\,E}{\mathcal{L}\,m\,{\omega_{\rm rf}}^2}\right)^2\,\sin\,2\Phi, \tag{A.15}$$

with solution

$$\begin{aligned} z' &= -\frac{1}{4\,c}\left(\frac{e\,E}{\mathcal{L}\,m\,{\omega_{\rm rf}}^2}\right)^2\,\cos\,2\Phi + \overline{z'}, \\ z &= -\frac{1}{8\,c}\left(\frac{e\,E}{\mathcal{L}\,m\,{\omega_{\rm rf}}^2}\right)^2\,\sin\,2\Phi + \overline{z'}\,\Phi\;, \end{aligned} \tag{A.16}$$

where a constant contribution to z has been dropped.

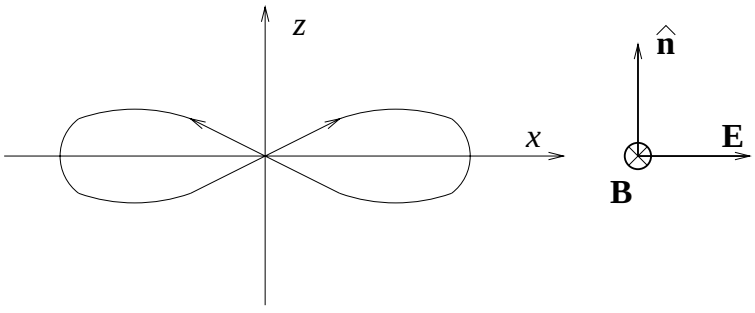

Figure A.1: Motion of electron, relative to its average motion, in a plane polarized, electromagnetic plane wave.

Energy transfer. Because the motion has a transverse component, parallel to the electric field, the particle energy varies;

$$\frac{d\gamma}{d\Phi} = \frac{e}{mc^2} \cdot \mathbf{v}' = \frac{1}{\mathcal{L}} \left(\frac{e\,E}{m\,c\,\omega_{\rm rf}} \right)^2 \sin\Phi, \quad \gamma = -\frac{1}{\mathcal{L}} \left(\frac{e\,E}{m\,c\,\omega_{\rm rf}} \right)^2 \cos\Phi + \gamma_0 \ . \qquad (A.17)$$

Any decrease of electron energy must correspondingly increase the beam energy. This is known as free electron laser radiation. If the wave increases the electron energy (at the expense of its own intensity) it is known as an inverse free electron laser. Whether the electron gains or loses energy depends on where it rides on the wave (i.e. its phase). Of course the laser cannot be arbitrarily long, since the phase varies monotonically, and the energy change eventually averages to zero. The considerations of this aside are not really relevant if the beam and wave are approximately anti-parallel, as is the case in the microwave undulator, since the phase Φ varies rapidly, and this averaging takes place almost instantly.

Comparison with undulator. Making the approximations $\Phi \approx 2\omega_{\rm rf} t$ and $\mathcal{L} \approx 2\gamma$, Eq. $(A.16)$ yields

$$\frac{dx}{d\,(ct)} = \frac{c\,E}{\gamma\ (m\,c^2/e)\,\omega_{\rm rf}} \sin\Phi \ . \qquad (A.18)$$

For comparison with undulator formulas, it is convenient to define an "effective K value"

$$K_{\rm eff.} = \frac{E}{m\,c^2/e} \frac{c}{\omega_{\rm rf}} \ , \qquad (A.19)$$

which is the maximum angle, expressed in units of $1/\gamma$.

Connection to microwave power. According to Eq. (4.2), the maximum electric field in a microwave beam is related to the beam power and other guide parameters by (factor of two standing wave, traveling wave ambiguity here)

$$P = \frac{|E_{\rm max}|^2}{Z_0} \sqrt{1 - \left(\frac{\lambda_{\rm rf}}{2a} \right)^2} \frac{ab}{2} \ . \qquad (A.20)$$

Combining Eqs. $(A.19)$ and $(A.20)$, $K_{\rm eff.}$ can be expressed as a product of dimensionless factors

$$K_{\rm eff.} = \frac{c}{\omega_{\rm rf}} \sqrt{\frac{2}{ab}} \left(1 - \left(\frac{\lambda_{\rm rf}}{2a} \right)^2 \right)^{-1/4} \sqrt{\frac{P}{(mc^2/e)^2\,/Z_0}} \approx \frac{1}{\sqrt{2}\,\pi} \frac{\lambda_{\rm rf}}{\sqrt{ab}} \sqrt{\frac{P\,({\rm MW})}{693.1\,{\rm MW}}} \ . \qquad (A.21)$$

Appendix B.
Is the Forward Peak Subject to Line Narrowing?

The $2N_w$ undulator pulses resemble the emission from a linear, phased array, transmitting antenna. Even though the individual elements in such an array radiate more or less isotropically, when they are phased correctly, a narrow beam parallel to the array can be produced. To produce such a beam with free-space wavelength λ, because the wavefronts propagate at the speed of light, successive radiators should be phase shifted by (an odd multiple of) $\pi\lambda_w/\lambda$ to give constructive interference in the direction parallel to the array. (We continue to use alternating sign radiators spaced at $\lambda_w/2$.) The angular width of the radiation pattern can be defined to be the angle of the first interference minimum. For emission at (small) angle ϑ there is a phase shift $N_w\lambda_w\theta^2\pi/\lambda$ between radiation from first and last radiators. The condition for the vanishing of the amplitude from all $2N_w$ radiators is that this phase shift be 2π. That is

$$\theta_{\min} = \sqrt{\frac{1}{N_w}}\sqrt{\frac{\lambda}{\lambda_w}} = \frac{1}{\gamma}\frac{1}{\sqrt{2N_w}} \ , \qquad (B.1)$$

where, in the last step, the relation $\lambda = \lambda_w/(2\gamma^2)$ has been used. This is indeed a small angle. Since, for large N_w, it is much smaller than the cone angle $1/\gamma$ characterizing radiation from a single radiator, it seems to imply that the gross angular radiation pattern (angular width of order $1/\gamma$) will exhibit circular fringes with spacing given by Eq. $(B.1)$. For $2N_w = 400$ there will be some 20 fringes.

The argument in the previous paragraph is fallacious however, since it assumed the radiation to be monochromatic, with wavelength independent of angle. In fact there is a large spread of wavelengths. At any angle the interference of all contributions at angle ϑ has already been accounted for in Eqs. (3.1) and Eq. (3.6). With Jackson, I therefore expect no fringes.

Even if such fringes existed I think that they would add little to the practical value of the beam as an X-ray source. For one thing, they would be washed out if the angular spread of the electron beam is comparable with $\theta_{\min}$ (as is likely to be the case). For another, only a small fraction of the flux would be present in the central maximum, so collimating down to select only the central peak seems to be not advisable. (It would

violate the maxim "Never give away flux for brilliance.") In any case, because the fringe widths and fringe separations are comparable, the local brilliance is not much greater than the average brilliance. The only practical exploitation I can imagine would be a special purpose X-ray diffraction analysis that could take advantage of the known, high resolution, coherent fringe structure of the beam. In this report I have assumed that the $1/\gamma$ angular spread characterizing emission from individual emitters is already small enough to provide motivation for the undulator being discussed. If the fringes exist, they are so narrowly spaced as to be insignificant.

These comments are certainly not intended to belittle the value of undulators in general. The narrowing proportional to $1/N_w$ of the frequency spectrum at fixed angle, say in the forward direction, is both uncontroversial and invaluable. It results in brilliance increasing as N_w^2.

Before leaving the question of whether fringes exist one can contemplate how such fringes might emerge from Jackson's, work-it-out-in-the-electron's-rest-system approach. For a start, one can question an assumption that is built into the Jackson picture, in spite of its being manifestly incorrect. I refer to the assumption that the electrons execute pure simple harmonic motion in their own rest frame when, in fact, they exhibit this motion only during the "time window" during which the wiggler is flying by. The width in time of this window is $\Delta T'_w = N_w L_w/(\gamma c)$. The dipole radiation due to this oscillation will therefore be gated on for a time interval of length $\Delta T'_w$. At any angle the fields will be the product of a pure sinusoid and a square pulse. The frequency domain spectrum will therefore be the convolution of a single line (from the sinuisoid) and a $(\sin\omega)/\omega$ spectrum (from the square pulse). Qualitatively, the rest system frequency will be spread over a range $\Delta\omega'_w \approx 1/\Delta T'_w$.

In the absence of the spread just described, the rest system dipole radiation is monochromatic; it is only after transformation back into the laboratory system that energy variation results and, even then, there is a one-to-one relation between frequency and angle. (This is because the laboratory system angle increases monotonically with increasing rest system angle.) At fixed laboratory angle the radiation is therefore not only monochromatic, but has unique phase. The presence of frequency spread in the electron's rest system changes this. Because of the spread of frequencies in the rest system there is the possibility of more

than one contribution to the radiation at fixed laboratory angle. For example, one visualizes two rest system photons having different rest system frequencies and angles, but the same lab system frequencies and angles, and which could therefore interfere constructively of destructively. Unfortunately this is impossible, since the angle transformation from rest system to laboratory is independent of frequency. Therefore the laboratory frequency spectrum is the same as the rest system frequency spectrum (except for the scale of the frequency axis.) Nothing in this picture seems to predict the existence of angular fringes in the forward radiation.

Yet one more point can be made. All analyses of undulator radiation seem to employ the Fraunhofer picture, in which the detector is "at infinity". This assumption can be validated either by the image distance being large relative to all relevant source dimensions or by the presence of a parallel-to-point focusing lens. For undulator sources neither of these possibilities is fully available. X-ray lenses don't exist and focusing mirrors are problematical. And, especially with long undulators, the ratio of detector distance to undulator length may not be very large. It seems fair to say, therefore, that X-ray detectors are "out of focus" for observing interference fringes. This is just one more way in which any supposed fringes would be washed out.

Appendix C.
Treatment of Magnetic Wiggler Radiation as Compton Scattering

C.1. Thomson Scatttering Treatment

There is a well-known treatment of undulator radiation as Compton back-scattering of the "photons" that are "produced" in a wiggler magnet. Since the frequency of these photons is zero, yet their wavelength is λ_w, they do not satisfy the relation between energy and momentum of *real* photons, and they are said to be *virtual*.

For a horizontal-bending undulator aligned with the z-axis, the only non-vanishing electric or magnetic field component is $B_y = B_0 \cos(k_w z)$. With electrons propagating at velocity $-v$ along the positive z-axis, it is useful to transform the wiggler field into the rest frame of the electron. The result is

$$\mathbf{E}' = -\gamma\, v\, B_y \cos\left(k_w \gamma \left(z' + vt'\right)\right)\, \hat{\mathbf{x}}, \quad \text{and} \quad \mathbf{B}' = -\frac{\mathbf{v}}{v^2} \times \mathbf{E}' \ . \tag{C.1.1}$$

This is very nearly the relation between $\mathbf{E}'$ and $\mathbf{B}'$ belonging to a plane-polarized plane wave, propagating in free space. In fact, in the limit $v \to c$ the correspondance becomes exact. Making the replacement $v = c$ yields what is known as the Weizsäcker-Williams approximation.

The wave just derived is said to be made up of "virtual" photons, and these photons can Compton scatter off the electrons. The (magnitude of) the rest energy of one of these virtual photons (calculated most easily in the laboratory frame, since the frequency vanishes there) is given by

$$|m_\gamma c^2| = \left|\sqrt{(\hbar\omega)^2 - (\hbar k_w)^2 c^2}\right| = \hbar k_w c \ . \tag{C.1.2}$$

Next consider the situation in the rest frame of the electrons. In this frame the photon energy is $E'_\gamma = \hbar k_w \gamma v$, since $k_w \gamma v$ is the (frequency) factor multiplying t' in the argument of the cosine factor in Eq. (C.1.1). If this energy is small compared to the electron rest energy,

$$E'_\gamma = \hbar k_w \gamma v << mc^2 \ , \tag{C.1.3}$$

(as will always be true for cases of interest to us) the incident and scattered photon energies are the same. It will be valid to neglect the virtual photon mass (calculated in Eq. $(C.1.2)$) if it is small compared to this energy;

$$\hbar k_w c \stackrel{?}{<<} \hbar k_w \gamma v \ , \qquad (C.1.4)$$

which reduces to $\gamma >> 1$, and will be abundantly true in practice.

Condition $(C.1.3)$ is also the condition for the validity of treating Compton scattering as Thomson scattering, for which the total cross section is

$$\sigma = \frac{8\pi}{3} r_e^2 = 0.665 \times 10^{-28}\,\mathrm{m}^2 \ . \qquad (C.1.5)$$

where $r_e = 2.81784 \times 10^{-15}$ m. (See Eq. (2.21).) Though this cross section was calculated in the electron rest frame, the lab frame value is the same.

To calculate the radiation pattern in the laboratory it is necessary to write the angular distribution in the rest system of the electron, and then to transform it into the laboratory system. Though the scattered photons are mono-energetic in the electron rest system, this will no longer be true in the laboratory system. We can write down the maximum lab energy, since it corresponds to pure back-scattering. The result of Lorentz transforming the photon four-vector, $(\hbar\gamma k_w c, 0, 0, \hbar\gamma k_w)$, back to the lab frame, is a photon of energy

$$E_\gamma = \left(1 + \frac{v}{c}\right) \gamma^2 \hbar k_w \ . \qquad (C.1.6)$$

Since $v \approx c$, the back-scattered wave length is less than the wiggler period λ_w by the factor $2\gamma^2$. This agrees with the undulator peak calculated using classical electrodynamics.

In the Thomson limit of Compton scattering, the rest system radiation from an electron is given by the classical dipole radiation formula. Since this is the formula that Jackson uses to calculate undulator radiation, it should be clear that a Thomson scattering treatment is equivalent to the Jackson treatment of radiation from a magnetic undulator.

C.2. Relativistically Invariant Treatment of the Microwave Undulator

Though the magnetic field of an undulator has been described as made up of photons, it is even more natural to treat a microwave beam this way, especially because the photons are real, not virtual. On the other hand, according to Eq. (4.3), the microwave photons are directed at angles $\pm\cos^{-1}\sqrt{1-(\lambda_{\rm rf}/(2a))^2}$ relative to the waveguide, and therefore also relative to the electron beam. Because of this, the electron-photon system has transverse momentum $p_{\perp,\gamma}$. This can be compared to the typical transverse momentum $p_{\perp,e}$ an electron has because of its betatron oscillation amplitude;

$$\frac{p_{\perp,\gamma}}{p_{\perp,e}} \approx \frac{h/\lambda_w}{\gamma m_e c\sqrt{\epsilon_x/\beta_x}} \quad \left(\stackrel{\text{e.g.}}{=} \frac{12.4\,\text{keV}}{2\gamma^3 \times 0.511\,\text{MeV}}\sqrt{\frac{\beta_x}{\epsilon_x}}\,. \right) \qquad (C.2.1)$$

This ratio is negligibly small for any conceivable electron beam. It is therefore legitimate to treat photon and electron as traveling on anti-parallel tracks. It may be important, later, to account for the spread of electron directions.

In this paper the polarization of the outgoing photons has been treated carelessly so far—only the in-plane polarization component has been retained, and only approximately at that. We are now in a position to tidy up this treatment, since the polarization dependence of Compton scattering is well documented. In the remainder of this section formulas will be copied from Berestetskii, Lifshitz, and Pitaevski, (BLP)[9] with considerably less than full understanding on my part. Feynman diagrams for the process are shown in Fig. C.2.1(a). Most formulas will be specialized to a frame of reference in which the accelerator is at rest.

Traditional discussions of Compton scattering have employed either electron rest system (sometimes called the "laboratory system), or a "center of mass" system in which the electron and photon momenta are equal and opposite. We will work in a different "laboratory system"; in it the photon is incident with four-momentum $\underline{k}$, traveling in the negative z-direction along the positive z-axis, and the electron is incident with four-momentum $\underline{p}$ traveling in the positive z-direction along the negative z-axis. With $\hbar = c = 1$, and

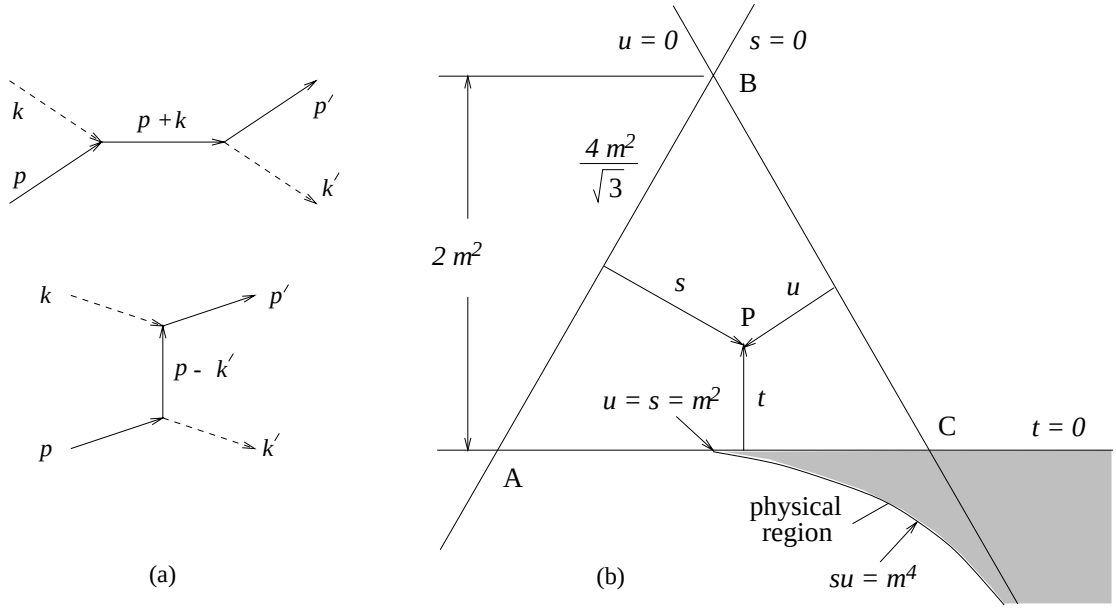

Figure C.2.1: (a) Feynman diagrams for Compton scattering. (b) Kinematic variables. Triangles APB, APC, and BPC have areas $(2/\sqrt{3})m^2 s$, $(2/\sqrt{3})m^2 t$, and $(2/\sqrt{3})m^2 s$, and triangle ABC has area $(4/\sqrt{3})m^4$ and is equal to their sum. This assures that Eq. $(C.2.6)$ is satisfied.

$E = \sqrt{p^2 + m^2}$, the initial four-momenta are†

$$\underline{k} = (\omega, -\omega, 0, 0) = (\omega, \mathbf{k}) \ , \quad \underline{p} = (E, p, 0, 0) = (E, \mathbf{p}) \ , \tag{C.2.2}$$

and the final four-momenta are

$$\underline{\omega'} = \left(\omega', k'_x, k'_y, k'_z\right) = \left(\omega', \mathbf{k}'\right) \ , \quad \underline{p'} = \left(E', p'_x, p'_y, p'_z\right) = \left(E', \mathbf{p}'\right) \ . \tag{C.2.3}$$

Representing invariant scalar products of 4-vectors a and b by

$$(\underline{a}, \underline{b}) \equiv a_0 b_0 - \mathbf{a} \cdot \mathbf{b} \ , \tag{C.2.4}$$

standard kinematic variables s, t, and u are defined by

$$\begin{aligned} s &= \left(\underline{p} + \underline{k}, \underline{p} + \underline{k}\right) = m^2 + 2\left(\underline{p}, \underline{k}\right) = m^2 + 2\omega\left(E + p\right) \ , \\ t &= \left(\underline{p} - \underline{p'}, \underline{p} - \underline{p'}\right) = -2\left(\underline{k'}, \underline{k}\right) = -2\omega\omega'\left(1 + \cos\vartheta\right) \ , \\ u &= \left(\underline{p} - \underline{k'}, \underline{p} - \underline{k'}\right) = m^2 - 2\left(\underline{p}, \underline{k'}\right) = m^2 - 2\omega'\left(E - p\cos\vartheta\right) \ . \end{aligned} \tag{C.2.5}$$

In the last steps, working in the laboratory system, with the photon scattering angle defined to be ϑ, the substitution $k'_x = \omega' \cos\vartheta$ has been performed.

† For consistency with Berestetskii, Lifshitz, and Pitaevski, the notation for the rest of this appendix is inconsistent with notation in the rest of the paper. The main inconsistencies are that the photon is incident from the right and the produced photon frequency, previously called ω, will, from here on, be ω'.

As illustrated in Fig. C.2.1, these variables satisfy

$$s+t+u=2m^2 \quad \text{or} \quad \frac{\omega}{\omega'}=\frac{E-p\cos\vartheta}{E+p}+\frac{\omega\,(1+\cos\vartheta)}{E+p}\approx\frac{1-(p/E)\cos\vartheta}{1+p/E}\ . \qquad (C.2.6)$$

Dropping the last term will always be valid in the present context. To confirm this, even at $\vartheta=0$, a useful number is

$$\frac{\omega E}{m^2}=\frac{\omega\gamma}{m}, \quad \left(\stackrel{\text{e.g.}}{=}\frac{1.24\times10^4\,\text{eV-Å}}{4\times10^8\,\text{Å}}\,\frac{10^4}{0.511\times10^6\,\text{eV}}=0.6\times10^{-6}\ .\right) \qquad (C.2.7)$$

For further simplifying Eq. $(C.2.6)$, one can employ $p/E\approx1-\gamma^2/2$ and $\cos\vartheta\approx1-\vartheta^2/2$, so that

$$\omega'(\vartheta)\approx2\omega\left(\frac{1}{2\gamma^2}+\frac{\vartheta^2}{2}\right)^{-1}\ . \qquad (C.2.8)$$

Recognizing from Eq. (1.2) that $\lambda_w\approx\lambda_{\rm rf}/2$, apart from notational differences, this relation is equivalent to Eq. (3.2) with $n=1$ and $\Delta\Theta=0$. One also obtains the approximation

$$t\approx-4\omega\omega'\approx-2\omega^2\,(1-(p/E)\cos\vartheta)\ . \qquad (C.2.9)$$

But it is not safe to evaluate u using the final (approximate) form of Eq. $(C.2.6)$, since this would yield the result that u is independent of ϑ, (and we will need a formula for $du/d\cos\vartheta$.) From the exact form of Eq. $(C.2.6)$ we have

$$\frac{d\omega}{d\cos\vartheta}=\frac{\omega'^2}{\omega}\,\frac{p-\omega}{E+p}\ . \qquad (C.2.10)$$

Differentiating the last of Eqs. $(C.2.5)$ then yields

$$\begin{aligned}\frac{du}{d\cos\vartheta}&=2\omega'p-2\omega'^2\left(\frac{p}{\omega}-1\right)\,\frac{E-p\cos\vartheta}{E+p}\\&=2\omega'p-2\omega'^2\left(\frac{p}{\omega}-1\right)\,\left[\frac{\omega}{\omega'}-\frac{\omega\,(1+\cos\vartheta)}{E+p}\right]\\&\approx\omega'^2\,(1+\cos\vartheta)\ .\end{aligned} \qquad (C.2.11)$$

BLP also define

$$\begin{aligned}x&=\frac{s-m^2}{m^2}=-\frac{2\omega\,(E+p)}{m^2}\ ,\\y&=\frac{m^2-u}{m^2}=\frac{2\omega'\,(E-p\cos\vartheta)}{m^2}\ .\end{aligned} \qquad (C.2.12)$$

For calculating the differential cross section (per solid angle element $d\Omega'$), the following relations follow from approximation $(C.2.9)$:

$$\begin{aligned}d\Omega'&=\sin\vartheta\,d\phi\,d\vartheta=-d\cos\vartheta\,d\phi\ ,\\dt\,d\phi&\approx2\omega^2\,d\cos\vartheta\,d\phi=-2\omega^2\,d\Omega'\ ,\\dy\,d\phi&\approx-\omega'^2\,(1+\cos\vartheta)\,d\cos\vartheta\,d\phi/m^2=\omega'^2\,(1+\cos\vartheta)\,d\Omega'/m^2\ .\end{aligned} \qquad (C.2.13)$$

Here ϕ is the azimuthal angle, which is the same in laboratory system, electron rest system, and center of mass system. For azimuthally symmetric cross sections, $d\phi$ can be replaced by 2π to obtain a cross section differential in $d\vartheta$.

For the case of all incident particles being unpolarized and summing over final state polarizations, BLP give the Compton differential cross section to be

$$\frac{d\overline{\sigma}}{d\Omega'} = -8r_e^2 \frac{\omega^2}{m^2x^2}\left(\left(\frac{1}{x}-\frac{1}{y}\right)^2 + \left(\frac{1}{x}-\frac{1}{y}\right) + \frac{1}{4}\left(\frac{x}{y}+\frac{y}{x}\right)\right) \ . \qquad (C.2.14)$$

In this formula, dt can be accurately approximated using Eq. $(C.2.9)$.

To analyse the polarization properties of the radiation one introduces photon polarization vector

$$\underline{e} = e_1\underline{e}_1 + e_2\underline{e}_2 \qquad (C.2.15)$$

where $\underline{e}_1$ and $\underline{e}_2$ are four-vectors with vanishing time parts and with the unit vectors $\mathbf{e_1}$ and $\mathbf{e_2}$ as spatial parts. These vectors are orthogonal to the photon direction and to each other, $\mathbf{e_1}\cdot\mathbf{e_2^*} = 0$, and $|e_1|^2$ and $|e_2|^2$ are probabilities that the photon has polarization $\overline{e}_1$ and $\overline{e}_2$ respectively. The state of polarization can be described by density matrix

$$\rho_{\alpha\beta} = e_\alpha e_\beta^* = \frac{1}{2}\begin{pmatrix} 1+\xi_3 & \xi_1 - i\xi_2 \\ \xi_1 + i\xi_2 & 1-\xi_3 \end{pmatrix} \ , \qquad (C.2.16)$$

where the ξ_1, ξ_2, ξ_3 are "Stokes parameters" that take values in the range from -1 to $+1$. It is unclear to me at the moment how to calculate the Stokes parameters corresponding to a mode propagating in a waveguide though, because the wave is completely polarized $\xi_1^2+\xi_2^2+\xi_3^2 = 1$. The simplest possibility (it seems to me) has, for the density matrix of the initial photon state,

$$\mathbf{e} = \hat{\mathbf{x}}, \quad \rho_{\alpha\beta} = \begin{pmatrix} 1 & 0 \\ 0 & 0 \end{pmatrix}, \quad (\xi_1,\xi_2,\xi_3) = (0,0,1) \ . \qquad (C.2.17)$$

This would correspond to a pure, linearly polarized wave propagating parallel to the waveguide axis, with electric field horizontal.

For unpolarized incident electrons, and summing over polarizations of the final electron, the polarization dependent cross section (which is the cross section we are interested in)

BLP give

$$\begin{aligned}\frac{d\sigma}{d\Omega'} &= \frac{1}{2}\frac{d\overline{\sigma}}{d\Omega'} + 2r_e^2\,\frac{\omega'^2\,(1+\cos\vartheta)}{m^2x^2}\,\Bigg(\left(\xi_3+\xi_3'\right)\left(-\left(\frac{1}{x}-\frac{1}{y}\right)^2-\left(\frac{1}{x}-\frac{1}{y}\right)\right)\\ &\quad+\xi_1\xi_1'\left(\frac{1}{x}-\frac{1}{y}+\frac{1}{2}\right)+\frac{\xi_2\xi_2'}{4}\left(\frac{x}{y}+\frac{y}{x}\right)\left(1+\frac{2}{x}-\frac{2}{y}\right)\\ &\quad+\xi_3\xi_3'\left(\left(\frac{1}{x}-\frac{1}{y}\right)^2+\left(\frac{1}{x}-\frac{1}{y}\right)+\frac{1}{2}\right)\Bigg)\\ &\equiv G_0+G_3\left(\xi_3+\xi_3'\right)+G_{11}\xi_1\xi_1'+G_{22}\xi_2\xi_2'+G_{33}\xi_3\xi_3'\ .\end{aligned}\qquad (C.2.18)$$

With coefficients defined this way, the Stokes parameters of the emitted photons are given by

$$\xi_1^{(f)}=\frac{G_{11}}{G_0+\xi_3G_3}\,\xi_1,\quad \xi_2^{(f)}=\frac{G_{22}}{G_0+\xi_3G_3}\,\xi_2,\quad \xi_3^{(f)}=\frac{G_3+G_{33}\xi_3}{G_0+\xi_3G_3}\ . \qquad (C.2.19)$$

According to this $\xi_1=\xi_2=0$ implies $\xi_1^{(f)}=\xi_2^{(f)}=0$ which, with $\xi_3=1$, implies $\xi_3^{(f)}=(G_3+G_{33})/(G_0+G_3)$.

References

1. D. Attwood, K. Halbach, and K. Kim, *Science*, **228**, 1265 (1985).
2. J.D. Jackson, *Classical Electrodynamics,* Third Edition, John Wiley, 1999.
3. M. Sands, *The Physics of Electron Storage Rings,* in International School of Physics, "Enrico Fermi", Academic Press, 1971.
4. R. Coisson, *On Synchrotron Radiation in Nonuniform Magnetic Fields*, Optics Communications, **22**, 135 (1977).
5. Bossart, *Observation of Visible Synchrotron Radiation Emitted by a High-Energy Proton Beam at the Edge of a Magnetic Field*, NIM, **164**, 375 (1979).
6. N. Marcuvitz, *Waveguide Handbook,* p. 58, McGraw-Hill, New York, 1951.
7. R.P. Walker, *Insertion Devices: Undulators and Wigglers*, in CERN 98-04, p. 156.
8. V.F. Suller, *Introduction to Current and Brightness Limits*, CERN 98-04, p. 89.
9. V. Berestetskii, E. Lifshitz, and L. Pitaevskii, *Quantum Electodynamics, Vol. 4 of Landau-Lifshitz*, Pergamon Press, 1982.